Received: 29 January 2023 | Revised: 19 June 2023 | Accepted: 27 June 2023

DOI: 10.1111/mmi.15125

RESEARCH ARTICLE

WILEY

Comparative proteomics of vesicles essential for the egress of *Plasmodium falciparum* gametocytes from red blood cells

Juliane Sassmannshausen[1] | Sandra Bennink[1] | Ute Distler[2] | Juliane Küchenhoff[1] | Allen M. Minns[3] | Scott E. Lindner[3] | Paul-Christian Burda[4,5,6] | Stefan Tenzer[2] | Tim W. Gilberger[4,5,6] | Gabriele Pradel[1]

[1]Division of Cellular and Applied Infection Biology, Institute of Zoology, RWTH Aachen University, Aachen, Germany

[2]Core Facility for Mass Spectrometry, Institute of Immunology, University Medical Centre of the Johannes-Gutenberg University, Mainz, Germany

[3]Department of Biochemistry and Molecular Biology, Huck Center for Malaria Research, The Pennsylvania State University, University Park, Pennsylvania, USA

[4]Centre for Structural Systems Biology, Hamburg, Germany

[5]Bernhard Nocht Institute for Tropical Medicine, Hamburg, Germany

[6]Biology Department, University of Hamburg, Hamburg, Germany

Correspondence
Gabriele Pradel, Division of Cellular and Applied Infection Biology, Institute of Zoology, RWTH Aachen University, Worringerweg 1, Aachen 52074, Germany.
Email: pradel@bio2.rwth-aachen.de

Funding information
Deutsche Forschungsgemeinschaft, Grant/Award Number: TE599/9-1, GI312/11-1, PR905/19-1 and PR905/15-1

Abstract

Transmission of malaria parasites to the mosquito is mediated by sexual precursor cells, the gametocytes. Upon entering the mosquito midgut, the gametocytes egress from the enveloping erythrocyte while passing through gametogenesis. Egress follows an inside-out mode during which the membrane of the parasitophorous vacuole (PV) ruptures prior to the erythrocyte membrane. Membrane rupture requires exocytosis of specialized egress vesicles of the parasites; that is, osmiophilic bodies (OBs) involved in rupturing the PV membrane, and vesicles that harbor the perforin-like protein PPLP2 (here termed P-EVs) required for erythrocyte lysis. While some OB proteins have been identified, like G377 and MDV1/Peg3, the majority of egress vesicle-resident proteins is yet unknown. Here, we used high-resolution imaging and BioID methods to study the two egress vesicle types in *Plasmodium falciparum* gametocytes. We show that OB exocytosis precedes discharge of the P-EVs and that exocytosis of the P-EVs, but not of the OBs, is calcium sensitive. Both vesicle types exhibit distinct proteomes with the majority of proteins located in the OBs. In addition to known egress-related proteins, we identified novel components of OBs and P-EVs, including vesicle-trafficking proteins. Our data provide insight into the immense molecular machinery required for the inside-out egress of *P. falciparum* gametocytes.

KEYWORDS
egress, gametocyte, malaria, *Plasmodium falciparum*, red blood cell, vesicle

1 | INTRODUCTION

The tropical disease malaria is caused by protozoan parasites of the genus *Plasmodium*. The disease is characterized by symptoms like high fever, anemia, nausea, and respiratory distress, mainly caused by the blood-infecting stages of the parasite. Approximately, 247 million infections and 619,000 deaths were claimed by malaria in 2021, with two-thirds of the victims being children younger than five years (World Health Organization, 2022). The majority of deaths by malaria is due to infections with *P. falciparum*, the causative agent of malaria tropica.

Transmission of malaria is vector-borne with *Plasmodium* parasites being spread from human to human by blood-feeding female *Anopheline* mosquitoes. In the human, the parasites follow an obligate intracellular lifestyle and reside within a parasitophorous

vacuole (PV) for most parts of their lifecycle. While vacuolar compartmentalization provides shelter for the parasites to protect themselves from the human immune system, the parasites eventually need to exit the enveloping cell to ensure lifecycle progression (reviewed in Flieger et al., 2018).

To exit the host cell, *Plasmodium* parasites initiate an orchestrated programme of molecular processes, which eventually result in membrane lysis (reviewed in, e.g., Bennink et al., 2016; Bennink & Pradel, 2021; Dvorin & Goldberg, 2022; Flieger et al., 2018; Sassmannshausen et al., 2020; Tan & Blackman, 2021; Wirth & Pradel, 2012). Host-cell exit has been particularly studied in the parasite blood stages, that is, the merozoites and the gametocytes. When egressing from the red blood cell (RBC), the two stages follow an inside-out mode, during which the PV membrane (PVM) ruptures prior to the RBC membrane (RBCM). In both blood stages, the egress cascade begins with the concurrent activation of the plasmodial guanylyl cyclase GCα and the cGMP-dependent protein kinase G following the perception of environmental signals. In accord with these events, the intracellular calcium levels rise, which among others results in the activation of various calcium-dependent protein kinases. The egress cascade eventually leads to the discharge of specialized secretory vesicles important for the rupture of PVM and RBCM.

In *P. falciparum* merozoites, egress-related vesicles, termed exonemes, release their content into the PV lumen to initiate RBC lysis. Among others, the exonemes contain the subtilisin-like protease SUB1 and the aspartic protease plasmepsin X (PMX). Once activated by PMX, SUB1 processes a variety of targets that are present in the PV, like the serine-repeat antigen proteins SERA5 and SERA6 as well as the merozoite surface protein MSP1, and these proteins are later required for destabilizing the RBC cytoskeleton prior to RBCM destruction as well as for mediating the invasion of a new RBC by the freshly released merozoites (Arastu-Kapur et al., 2008; Collins et al., 2017; Mukherjee et al., 2023; Nasamu et al., 2017; Ruecker et al., 2012; Silmon de Monerri et al., 2011; Stallmach et al., 2015; Tan et al., 2021; Thomas et al., 2018; Yeoh et al., 2007).

Vesicle-mediated exocytosis also plays a crucial role during the egress of gametocytes from RBCs. RBC lysis is mandatory for the gametocytes to finalize gametogenesis, once they have been activated in the mosquito midgut by environmental factors. Specialized vesicles of gametocytes, the osmiophilic bodies (OBs), cluster underneath the gametocyte plasma membrane (GPM) and discharge their content into the PV lumen within a minute following activation (Sologub et al., 2011). OBs were first described as electron-dense vesicles in electron micrographs of female gametocytes (Sinden, 1982); later also male OBs (MOBs) have been reported in *P. berghei*, which exhibit a different protein repertoire and a smaller morphology than the female OBs (Olivieri et al., 2015). A variety of proteins have previously been described that are located in the OBs and released into the PV, the first of which was the female-specific G377 (Alano et al., 1995; de Koning-Ward et al., 2008; Olivieri et al., 2015; Severini et al., 1999; Suárez-Cortés et al., 2016). Two other proteins, MDV1 (male development gene 1; also termed protein of early gametocytes 3, Peg3) and GEST (gamete egress and sporozoite traversal) have been shown to be present in OBs, with MDV1 additionally associating with PVM and GPM. Both proteins, MDV1 and GEST, are linked to PVM rupture during *P. berghei* gametogenesis (Furuya et al., 2005; Olivieri et al., 2015; Ponzi et al., 2009; Silvestrini et al., 2005; Suárez-Cortés et al., 2016; Talman et al., 2011). Moreover, the *P. berghei* gamete egress protein GEP and the putative pantothenate transporter PAT localize to OBs and mutants lacking GEP or PAT are unable to egress from the RBC (Andreadaki et al., 2020; Kehrer, Singer, et al., 2016). In addition, several proteases are present in the OBs, like the subtilisin-like protease SUB2 and the dipeptidyl aminopeptidase DPAP2 (Suárez-Cortés et al., 2016). Further, SUB1 and the aspartyl protease MiGS (microgamete surface protein) have been described as MOB-specific proteases, and deficiencies of SUB1 or MiGS result in impaired male gametogenesis (Pace et al., 2019; Suárez-Cortés et al., 2016; Tachibana et al., 2018).

Following secretion of the OB content into the PV lumen, the PVM ruptures at multiple sites before it breaks down into multilayered vesicles (MLV; Sologub et al., 2011). Subsequently, another vesicle-resident protein is discharged from the activated gametocyte, the *Plasmodium* perforin-like protein PLP2 (PPLP2; Deligianni et al., 2013; Sologub et al., 2011; Wirth et al., 2014). Once secreted, PPLP2 perforates the RBCM, resulting in membrane destabilization and the release of the RBC cytoplasm, while gametocytes deficient of PPLP2 remain trapped in the RBC upon activation. A time-span of roughly six minutes was monitored between exocytosis of the OBs and the PPLP2-positive vesicles, indicating that they are two different types of egress vesicles, which act one after the other. Following secretion of PPLP2, it requires another four minutes until the RBC lyses and fully formed gametes are released into the midgut lumen (Andreadaki et al., 2018; Sologub et al., 2011; Wirth et al., 2014).

The data obtained to date point to at least two types of vesicles that are involved in the egress of activated gametocytes from the RBC, that is, the OBs and the PPLP2-positive egress vesicles (in the following termed P-EVs). We here aimed to study the dynamics of the OBs and P-EVs during gametogenesis, to unveil their characteristic components and to identify novel secreted mediators of RBC egress.

2 | RESULTS

2.1 | OBs and P-EVs differ in their subcellular localization as well as time-point and calcium-dependency of discharge

To probe into similarities and differences of OBs and P-EVs during gametocyte egress, we first used immunohistochemical methods to define their subcellular localization and order of discharge. For vesicle visualization, the OB proteins G377 and MDV1 and the P-EV-resident PPLP2 were chosen. All the three proteins display a signal peptide; in addition, PPLP2 possesses an MACPF domain essential for the pore-forming ability (Figure 1a).

Indirect immunofluorescence assays (IFAs) were employed to determine the subcellular localization of G377, MDV1, and PPLP2,

using specific antisera from rat, rabbit, and mouse. All of the proteins were detected in the cytoplasm of wildtype (WT) NF54 gametocytes, localizing to vesicular structures (Figure 1b; Figure S1a–c). Both MDV1 and G377 were found in vesicles that are particularly located at the periphery of the gametocytes; PPLP2 was further detected in vesicles rather accumulating in the central parts of the cell. In accord with previous reports (Deligianni et al., 2013; Severini et al., 1999; Silvestrini et al., 2005; Wirth et al., 2014), G377 and MDV1 are specific for gametocytes and expressed during gametocyte maturation, whereas PPLP2 is present in both the asexual and sexual blood stages (Figure S1a–c).

Colabeling IFAs confirmed a colocalization of the two OB-resident proteins G377 and MDV1, while the PPLP2 signal did neither overlap with the one of G377 nor of MDV1 (Figure 1b). No labeling was observed when the gametocytes were immunolabeled with serum of non-immunized mice, rats, or rabbits (Figure S2a). Colocalization of the signals were statistically quantified for each double-labeling experiment by calculating the Pearson's correlation coefficient (PCC). The signal patterns of G377 and MDV1 exhibited a PCC of 0.61, while the PCCs of PPLP2 with G377 or MDV1 showed values of 0.24 and 0.35 (Figure 1c), indicating that the PPLP2-containing P-EVs are different from the G377- and MDV1-positive OBs.

To investigate the time-points of discharge for the two vesicle types, WT NF54 gametocytes were activated and samples were taken at several time points between 0 and 20 min post-activation. Subsequently, the two vesicle types were highlighted by immunolabeling of either G377 or MDV1 and of PPLP2, using the respective antisera. While the signal for the OB-resident G377 disappeared within 2 min post-activation, the PPLP2-containing P-EVs could be detected for another 10 min, during which the P-EVs relocated from the center to the periphery of the gametocytes (Figure 1d). Around 15 min post-activation, the PPLP2 signal disappeared. Similarly, the OB-specific signals for MDV1 relocated to the gametocyte periphery within 2 min post-activation and were later seen associated with the plasma membrane of the newly formed gametes (Figure S2b).

In addition, we determined the role of intracellular calcium as a potential mediator of vesicle discharge. WT NF54 gametocytes were activated in the absence or presence of 25 μM of the selective calcium chelator BAPTA–AM and samples were taken between 0 and 20 min post-activation. The samples were then subjected to IFA, using anti-PPLP2 and anti-G377 antisera to highlight the two vesicle types (Figure S3a). In gametocytes not treated with BAPTA–AM, we again observed that the G377 signal of the OBs disappeared within less than 5 min post-activation, while the PPLP2 signal indicative of P-EVs relocated to the gametocyte periphery and then disappeared between 10 and 20 min post-activation. When the gametocytes were treated with BAPTA–AM prior to activation, the PPLP2-positive P-EVs were still detectable at 20 min post-activation, indicating that they were unable to discharge, whereas for G377, no difference in the labeling pattern compared with the untreated control was observed. The experiment was repeated using antibodies directed against Pfs16 and human spectrin to visualize PVM and RBCM, respectively. As observed before, the G377-positive signal disappeared independently of BAPTA–AM treatment. Concurrently with the disappearance of G377, the Pfs16-positive PVM vanished and in some cases minor dots were visible, which most likely represented MLVs (Figure S3b). Furthermore, the enveloping RBC highlighted by spectrin labeling disappeared and only RBCM remnants were detectable. PPLP2 was still detectable 20 min post-activation, when the gametocytes were treated with BAPTA–AM, but the Pfs16 signal disappeared with the exception of some dots, indicating that PVM breakdown into MLVs occurred independent of BAPTA–AM treatment. As expected, the spectrin-positive RBCM remained intact, when the activated gametocytes were treated with BAPTA–AM, due to the impaired discharge of PPLP2 (Figure S3b). For quantification, the presence or absence of the PPLP2 and G377 signals at 20 min post-activation was determined in 50 activated rounded gametocytes per experimental setting (Figure 1e). While the proportion of G377-positive cells was equally low in the presence or absence of BAPTA–AM (18% and 21%, respectively), a significant difference was observed in the proportion of PPLP2-positive cells, which varied between 15% in untreated and 54% in BAPTA–AM-treated gametocytes (Figure 1e).

Our combined data demonstrate that OBs and P-EVs are different types of vesicles, which discharge at different time points post-activation with the exocytosis of the OBs preceding discharge of the P-EVs. Further, we showed that exocytosis of the P-EVs, but not of the OBs, is sensitive to the calcium chelator BAPTA–AM, indicating its dependency on intracellular calcium.

2.2 | OBs and P-EVs exhibit distinct proteomes with multiple constituents

In order to identify constituents of the OBs and P-EVs, transgenic parasite lines were generated that express the proteins G377, MDV1, or PPLP2 fused to the promiscuous *E. coli* biotin ligase BirA, which allows the identification of proximal proteins by biotinylation (BioID; e.g., Roux et al., 2018).

For BioID analyses of putative PPLP2 interactors, a parasite line was generated that episomally expresses PPLP2 fused to BirA and green fluorescent protein (GFP), using the vector pARL-PPLP2-*pffnpa*-GFP-BirA, which expresses the fusion protein under the control of the *pffnpa* promoter (Figure S4a; Musabyimana et al., 2022). Furthermore, transgenic lines that endogenously express G377 or MDV1 fused to the enhanced TurboID version of BirA in addition to GFP were generated via homologous recombination using vectors pSLI-G377-TurboID-GFP and pSLI-MDV1-TurboID-GFP, respectively (Figure S4b; Branon et al., 2018). The episomal presence of vector pARL-PPLP2-*pffnpa*-GFP-BirA in the transgenic parasites and the successful integration of the vectors pSLI-G377-TurboID-GFP and pSLI-MDV1-TurboID-GFP into the respective *g377* or *mdv1* gene loci was demonstrated by diagnostic PCR (Figure S4c,d).

Western blot analyses of gametocyte lysates prepared from the transgenic lines, using mouse anti-GFP antibody, demonstrated the expression of the respective fusion proteins (Figure S5a). The

proteins MDV1-TurboID-GFP and G377-TurboID-GFP migrated at the expected molecular weights of 91 and 439 kDa, respectively. For PPLP2, a band of approximately 120 kDa was detected in addition to the expected band of 187 kDa, indicating processing of the protein. No protein bands were detected in lysates of either the asexual blood stages of the transgenic lines nor of WT NF54 mixed asexual blood stages and gametocytes (Figure S5a). Similarly, immunolabeling with anti-GFP antibodies demonstrated the expression of PPLP2-GFP-BirA, MDV1-TurboID-GFP, and G377-TurboID-GFP proteins in gametocytes of the respective transgenic lines and confirmed the presence of the tagged fusion proteins in vesicular structures (Figure 2a). In WT NF54 parasites, no GFP-labeling was detected.

Subsequent Western blotting was employed to highlight biotinylated proteins in the transgenic lines. For this, gametocyte cultures of each line were treated with 50 µM biotin for 15 min (TurboID) or 20 h (BioID). Immunoblotting of the respective gametocyte lysates using streptavidin conjugated to alkaline phosphatase detected multiple protein bands indicative of biotinylated proteins, including protein bands of 91, 187, and 439 kDa, likely representing the biotinylated fusion proteins MDV1-TurboID-GFP, PPLP2-GFP-BirA, and G377-TurboID-GFP, respectively (Figure 2b). In gametocytes of the transgenic lines that were not treated with biotin, minor protein bands were detected, indicating that endogenous biotin has been present in the gametocyte cultures, which triggered the activity of the biotin ligase. No biotin-positive protein bands were detected in WT NF54 samples (Figure 2b). IFA analyses of biotin-treated gametocytes of the transgenic lines, using fluorophore-conjugated streptavidin, confirmed the presence of biotinylated proteins, which localized in vesicular structures, while no biotinylated proteins were detected in biotin-treated WT NF54 gametocytes (Figure S5b).

BioID analyses were subsequently employed to analyze the proteomes of the OBs and P-EVs of *P. falciparum*. For this, gametocytes of the respective transgenic lines were treated with biotin as described above, and equal amounts of gametocytes per sample were harvested. Three independent samples were collected from each of the three lines (MDV1-TurboID-GFP, G377-TurboID-GFP, and PPLP2-GFP-BirA); two additional independent samples from the PPLP2-GFP-BirA line were included. Mass spectrometric analysis was performed on streptavidin-purified protein samples with three technical replicas for each sample. This resulted in the identification of 636 (MDV1-TurboID-GFP), 189 (G377-TurboID-GFP), and 298 (PPLP2-GFP-BirA) significantly enriched proteins, respectively (Figure 3a; Table S1). For each transgenic parasite line, the respective bait protein, that is, G377, MDV1, and PPLP2 was detected among these proteins (marked in Table S1). The initial list of significantly enriched proteins was subjected to two curation steps. In a first step, proteins without a putative signal peptide and/or transmembrane domains or with C-terminal ER retention signals were excluded, reducing the potential interactors to 169 proteins (MDV1-TurboID-GFP), 50 proteins (G377-TurboID-GFP), and 64 proteins (PPLP2-GFP-BirA) (Figure 3a; Table S2). In a second step, proteins with defined known functions not related to OBs or P-EVs (e.g., nucleoporins, chaperons) were removed from the list, eventually resulting in the following numbers of putative proteins of egress vesicles (gametocyte egress vesicle proteins, GEVPs): 132 proteins (MDV1-TurboID-GFP), 38 proteins (G377-TurboID-GFP), and 44 proteins (PPLP2-GFP-BirA; Figure 3a; Table S2).

Firstly, we determined, how many interactors were shared by the three bait proteins. After subtracting out protein multiplications, we obtained a total of 143 individual GEVPs. The comparison of GEVPs by bait proteins identified 13 proteins as putative interactors of both OB proteins, G377 and MDV1. It also revealed 16 proteins as putative interactors of MDV1 and PPLP2, while only 2 proteins were shared between G377 and PPLP2 (Figure 3b; Table S2). Further, 20 proteins were shared between three bait proteins. This group of proteins included, in addition to the three bait proteins, among others five members of the LCCL-domain protein family, as well as P230, hence, adhesion proteins known to locate in the PV of gametocytes, where they form protein complexes that are linked to the GPM (Simon et al., 2009, 2016; reviewed in Kuehn et al., 2010).

The 143 putative GEVPs were then grouped by predicted function (Figure 3c). The majority of GEVPs belonged to the categories of protein trafficking, processing and adhesion as well as transmembrane transport (~10% in each category). A total of 8% of GEVPs was previously assigned to host cell exit, for example, EPF1 (exported

FIGURE 1 Colocalization and dynamics of egress vesicles during gametocyte activation. (a) Schematic of the proteins MDV1, G377, and PPLP2. SP, signal peptide; MACPF, Membrane Attack Complex/Perforin domain. (b) Vesicular localization of MDV1, G377, and PPLP2 in gametocytes. WT NF54 gametocytes were immunolabeled with rabbit anti-G377, rat anti-MDV1 and mouse anti-PPLP2 antisera (red and green) to investigate co-localization of the respective proteins. Parasite nuclei were highlighted by Hoechst 33342 nuclear stain (blue). Bar; 2 µm. DIC, differential interference contrast. Details on the vesicular localization in blood stage parasites are provided in Figure S1a–c. Corresponding negative controls are provided in Figure S2a. (c) Quantification of protein colocalization. The PCC was calculated using Fiji ImageJ2. Immunolabeling of G377 or MDV1 was defined as region of interest ($n = 50$). The error bars indicate mean ± SD. (d) Dynamics of G377- and PPLP2-positive vesicles during gametocyte activation. WT NF54 gametocytes were collected at 0–20 min post-activation (p.a.) and immunolabeled, using rabbit anti-G377 or mouse anti-PPLP2 antisera (green). Gametocytes were counterstained with rabbit or mouse anti-P230 antisera (red). Parasite nuclei were highlighted by Hoechst 33342 nuclear stain (blue). Bar; 2 µm. NRBS, neutral rabbit serum; NMS, neutral mouse serum. The dynamics of MDV1-positive vesicles are shown in Figure S2b. (e) Calcium-dependency of vesicle discharge following gametocyte activation. WT NF54 gametocytes were treated with 25 µM BAPTA–AM prior to activation and immunolabeled with as described in (d). Untreated gametocytes served as control. A total of 50 activated (rounded) gametocytes per setting were evaluated for the presence of the G377 or PPLP2 signal at 20 min p.a. ($n = 3$). Corresponding IFA images are provided in Figure S3a. Information on membrane rupture during vesicle discharge are found in Figure S3b. The error bars indicate mean ± SD. ***$p \leq 0.001$ (One-Way ANOVA with Post-Hoc Bonferroni Multiple Comparison test; c, e). Results (b, d) are representative of three independent experiments.

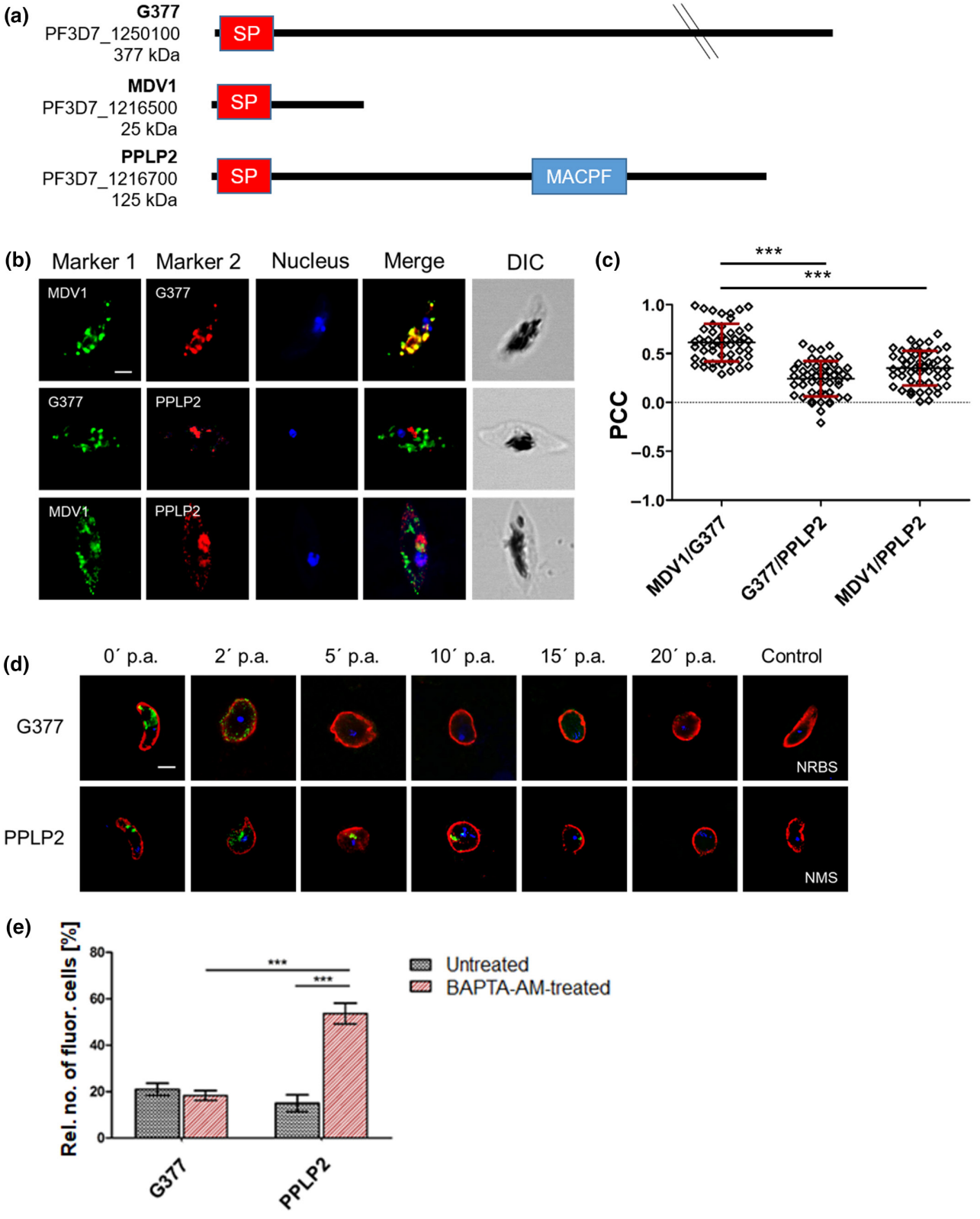

protein family 1), GEP (gamete egress protein), GEXP02 (gametocyte exported protein 2), PMX (plasmepsin X), SUB2 (subtilisin-like protease 2), MiGS (microgamete surface protein), and GEST (gamete egress and sporozoite traversal protein; e.g., Andreadaki et al., 2020; Grasso et al., 2022; Kehrer, Frischknecht, et al., 2016; Mbengue et al., 2013; Nasamu et al., 2017; Suárez-Cortés et al., 2016; Tachibana et al., 2018; Talman et al., 2011). Furthermore, 35% of GEVPs are of unknown function. An additional gene ontology (GO) term analysis revealed main molecular functions in peptidase activities and pyrophosphate hydrolysis as well as transmembrane

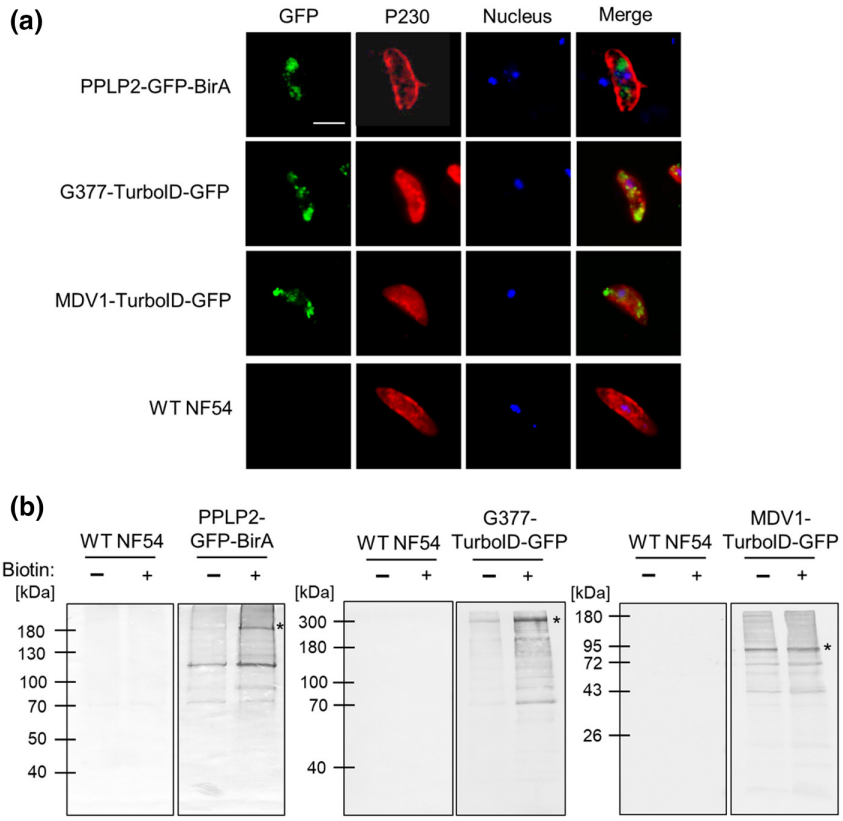

FIGURE 2 Verification of the parasite lines to be used in BioID. (a) Localization of the bait proteins in the BioID parasite lines. Gametocytes of lines PPLP2-GFP-BirA, G377-TurboID-GFP, and MDV1-TurboID-GFP were immunolabeled with mouse anti-GFP antibody to highlight PPLP2, G377 and MDV1, fused to GFP and biotin ligase (green). Gametocytes were counterstained with anti-P230 antisera (red); parasite nuclei were highlighted by Hoechst 33342 nuclear stain (blue). WT NF54 gametocytes served as a control. Bar; 5 µm. (b) Protein biotinylation in the BioID parasite lines. Gametocytes of lines PPLP2-GFP-BirA, G377-TurboID-GFP and MDV1-TurboID-GFP were treated with biotin for 20 h (PPLP2-GFP-BirA) and 15 min (G377-, MDV1-TurboID-GFP). Untreated parasite lines and biotin-treated and untreated WT NF54 gametocytes served as controls. Gametocyte lysates were subjected to Western blot analysis and biotinylated proteins were detected using streptavidin-conjugated alkaline phosphatase. (+), treated with biotin; (−), untreated. Asterisks (*) highlight the bait proteins. Cloning strategy and transfection verification are provided in Figure S4. Further information on verification of the BioID lines is provided in Figure S5. Results (a, b) are representative of three independent experiments.

transport, and cellular localizations in host cellular components and vesicles (Figure S6a,b).

A comparative transcriptional analyses of the GEVPs (according to table "Transcriptomes of 7 sexual and asexual life stages"; López-Barragán et al., 2011; see PlasmoDB database; Aurrecoechea et al., 2009) showed that the majority of the proteins exhibited peak expression in stage V gametocytes and in ookinetes or in ring stages and trophozoites (Figure 3d), suggesting that they represent two groups of proteins, either expressed in the late stages of the sexual phase or during intraerythrocytic replication. When the sex specificity of the GEVPs was evaluated (according to table "Gametocyte Transcriptomes"; Lasonder et al., 2016; see PlasmoDB database; Aurrecoechea et al., 2009), roughly one-third of proteins are predominantly present in either male or female gametocytes, while one third of proteins did not exhibit any sex-specific transcript expression (Figure S6c).

The GEVPs were further subjected to STRING-based analyses to investigate the protein–protein interaction networks (see string-db.org; text mining included). Three main clusters were identified (Figure 4; Table S3). The first cluster involved proteins previously shown to form multi-adhesion domain protein complexes like the LCCL-domain (CCp) proteins, P48/45, and P230, plus the paralogs P47 and P230p (Pradel et al., 2004; Scholz et al., 2008; Simon et al., 2009, 2016; reviewed in Kuehn et al., 2010; Pradel, 2007). Furthermore, the cluster included three members of the PSOP (putative secreted ookinete protein) family, PSOP1, PSOP12, and PSOP13 (Ecker et al., 2008; Sala et al., 2015; Tachibana et al., 2021) and proteins linked to the PVM, that is, Pfs16, Pfg17-744, and Pfg14-748 (Bruce et al., 1994; Eksi et al., 2005). In addition, the three bait proteins G377, MDV1, and PPLP2, were found in this cluster. Noteworthy, the majority of proteins in this cluster were interactors of all three bait proteins.

A second cluster comprised proteins linked to vesicle biogenesis, particularly transmembrane transporters including the previously described ABCG2 transporter of female gametocytes (Tran et al., 2014). Further, the vesicle trafficking-related protein clathrin (heavy chain) and sortilin were found in this cluster (Figure 4; Table S3). Four of the proteins of this cluster belonged to the group of PPLP2 interactors.

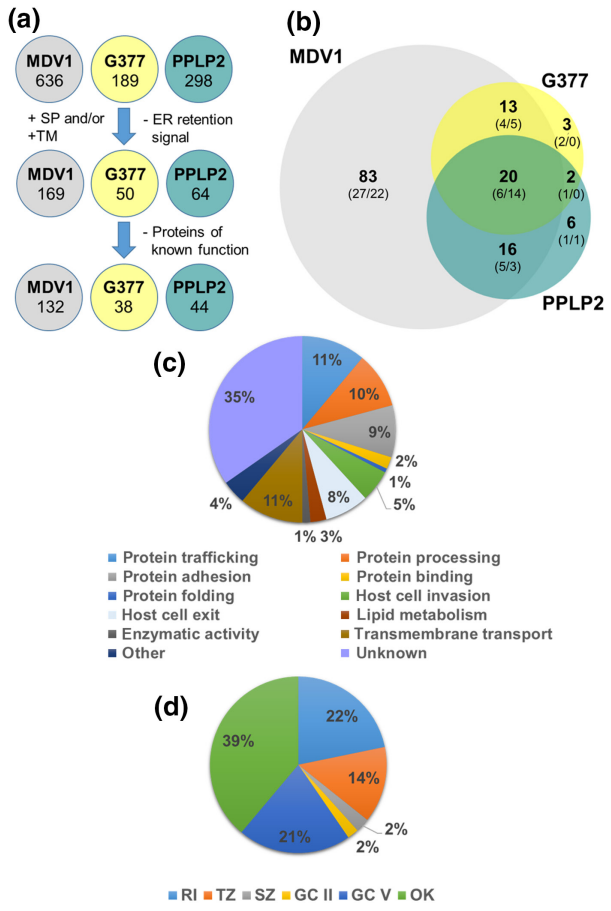

FIGURE 3 *In silico* analysis of the egress vesicle proteomes. (a) Schematic of candidate selection. Putative interactors of MDV1, G377, and PPLP2 following BioID of lines MDV1-TurboID-GFP, G377-TurboID-GFP and PPLP2-GFP-BirA were subjected to domain and functional analysis, resulting in the identification of a total of 143 individual GEVPs. Signal peptides (SP) were predicted using SignalP 4.1 & 5.0, transmembrane domains (TM) were predicted using DeepTMHMM, and endoplasmic reticulum (ER) retention signals were predicted using DeepLoc 2.0 and compared with a bioinformatic analysis of Külzer et al. (2009). Functional prediction was performed via PlasmoDB. (b) Venn diagram depicting the 143 GEVPs grouped by bait protein. The final numbers of interactors for each parasite line are depicted in bold, the predicted relative sex specificity is indicated (male/female; Lasonder et al., 2016; see PlasmoDB database). (c) Pie chart depicting the GEVPs (percentage of total numbers) according to predicted molecular function. (d) Pie chart depicting the GEVPs (percentage of total numbers) grouped by stages of peak expression (López-Barragán et al., 2011; see PlasmoDB database). RI, ring stage; TZ, trophozoite; SZ, schizont; GC II, gametocyte stage II; GC V, gametocyte stage V; OK, ookinete. Detailed information on the interactors before and after the application of selection criteria is provided in Tables S1 and S2. Further analysis of the GEVPs are provided in Tables S4 and S5. The corresponding GO term and sex specificity analyses are provided in Figure S6.

The third cluster resembled a megacluster that comprised various proteins particularly linked to RBC invasion and modification. Within the megacluster, two subclusters were distinguished, one of which included proteins linked to the Maurer's clefts, while the other one comprised proteins linked to rhoptries and micronemes. Additional proteins were associated with these subclusters, several of which are proteases, for example, SUB2, the dipeptidyl aminopeptidases DPAP1 and DPAP2, the metalloprotease M16, and the plasmepsins PMI, PMIII, and PMX, as well as the cysteine protease inhibitor falstatin (e.g., Banerjee et al., 2002; Boysen & Matuschewski, 2013; Child et al., 2013; Collins et al., 2020; Coombs et al., 2001; Klemba et al., 2004; Pandey et al., 2006; Tanaka et al., 2013; Uzureau et al., 2004). Furthermore, known components of the merozoite surface like GAMA, MaTrA, MSP8, or P38 as well as various exported proteins like GEXP08, GEXP21, EXP1, and EXP3 were found within the megacluster (Figure 4, Table S3; Arumugam et al., 2011; Black et al., 2005; Fischer et al., 1998; Hinds et al., 2009; Mesén-Ramírez et al., 2016, 2019; Ntumngia et al., 2004; Sanders et al., 2005; Silvestrini et al., 2010; Simmons et al., 1987; Vincensini et al., 2008). Since the majority of the megacluster proteins were previously linked to rings and trophozoites, they may have functions in both the asexual and sexual blood stages.

In a next step, we compared our data with results from previous proteomics studies, that is, three secretome analyses of activated *P. berghei* and *P. falciparum* gametocytes (Grasso et al., 2020, 2022; Kehrer, Frischknecht, et al., 2016), a BioID-based OB proteome study on *P. berghei* gametocytes using MDV1 as bait (Kehrer, Frischknecht, et al., 2016) and a comparative proteome study on G377-deficient *P. falciparum* gametocytes (Suárez-Cortés et al., 2016). A total of 32 GEVPs that were identified by us were also found in at least one of these studies, which include DPAP1, DPAP2, GAMA, GEST, MiGS, PMIX, PMX, PTEX150, PSOP1, PSOP12, and SUB2 (Tables 1 and S4). In addition, we examined if any of the GEVPs of our study are considered as putative SUB2 substrates, referring to a previous study on SUB2 and its substrates in *P. falciparum* merozoites (Collins et al., 2020). We noted 56 GEVPs that are potential SUB2 substrates, including GAMA, GEXP02, DPAP1, PMIV, PMX, and PTEX150, and the vast majority of these proteins are components of the OBs (Tables 1 and S5).

The fact that several known proteins where found in both the OB and P-EV interactomes suggests that these may have met during endomembrane trafficking. Exemplary, we investigated the vesicular localization of CCp2, a component of the multi-adhesion domain protein complex known to be synthesized continuously and present at the GPM (reviewed in Kuehn et al., 2010; Pradel, 2007). CCp2 as well as other components of the multi-adhesion domain protein complex have been identified as interactors of all three bait proteins (see above). IFA analyses confirmed the presence of CCp2 in vesicles and in association with the GPM as well as the plasma membrane of gametes, where it neither co-localizes with G377 nor PPLP2 (Figure S7).

In summary, we identified various proteins as potential constituents of egress vesicles. Among the candidates, previously described components of OBs and P-EVs as well as novel proteins were found. Novel candidates particularly included peptidases, transmembrane transporters, and proteins involved in vesicle trafficking. The vast majority of the identified GEVPs could be assigned to the OBs.

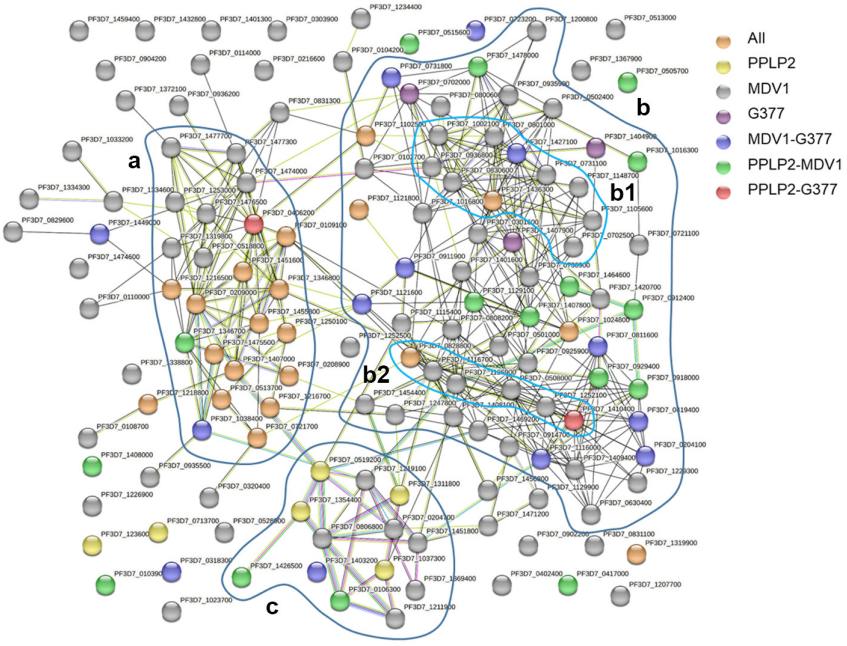

a - Adhesion protein/LCCL domain protein cluster
b - RBC invasion & modification cluster (b1: Maurer´s clefts subcluster; b2: Rhoptry & microneme subcluster)
c - Vesicle biogenesis cluster

FIGURE 4 Network analysis of GEVPs. The 143 GEVPs were evaluated for potential interactions using the STRING database. Based on the interaction among the query proteins, different functional clusters were identified. (a) Adhesion protein/LCCL-domain protein cluster with 23 proteins; (b) the RBC invasion and modification cluster with 59 proteins, including (b1) the Maurer's clefts subcluster and (b2) the rhoptry/microneme subcluster; (c) the vesicle biogenesis cluster of 13 proteins. Detailed information on individual proteins clustering in each subnetwork is provided in Table S3.

2.3 | Selected putative constituents localize to vesicular structures in gametocytes

Out of the 143 putative constituents of egress vesicles, six proteins previously not studied in gametocytes were chosen for further validation, that is, the Sel1-repeat containing protein (PF3D7_0204100), the putative secreted ookinete protein PSOP1 (PF3D7_0721700) and an unknown conserved protein, here termed GEVP1 (PF3D7_0811600), all of which interact with G377 and MDV1, the PPLP2-interacting v-SNARE protein Vti1 (PF3D7_1236000) of P-EVs, and the GPI-anchored micronemal antigen GAMA (PF3D7_0828800) and an unknown conserved protein, here termed GEVP2 (PF3D7_1319900), which were identified as interactors of G377, MDV1, and PPLP2. Transgenic lines were generated, using vector pSLI-HA-*glmS* (Musabyimana et al., 2022), which enables the expression of the protein of interest fused to a hemagglutinin A (HA)-tag, while the respective transcript is merged with the *glmS* ribozyme in the 3′ untranslated region (Figure S8a). Successful vector integration into the targeted locus was shown by diagnostic PCR (Figure S8b).

Western blotting of lysates derived from all of the six HA-tagged parasite lines confirmed their expression in the *P. falciparum* blood stages. Five of the HA-tagged proteins were detected in lysates of both asexual blood stages and gametocytes, running at the expected molecular weights, that is, Sel1 (271 kDa), PSOP1 (53 kDa), GEVP1 (144 kDa), GAMA (86 kDa), and Vti1 (49 kDa; Figure 5a). GEVP2 was restricted to gametocyte lysates and in addition to the expected 179 kDa protein, a second band running at approximately 120 kDa was identified, indicating protein processing. No protein bands were detected in lysates of WT parasites, which served as a control (Figure 5a).

The subcellular localization of the HA-tagged proteins in gametocytes was investigated by IFAs. All of the proteins showed a punctuate localization within the gametocyte cytoplasm, clearly defining vesicular structures (Figure 5b). In addition, the localization of these vesicles in the context of OBs and P-EVs was investigated by colabeling experiments. IFAs demonstrated colabeling of PSOP1 and GEVP1 with G377, indicating their localization in OBs. No clear colocalization with G377 or PPLP2, however, was observed for HA-tagged Sel1, GAMA, Vti1, and GEVP2 (Figure S9a). Immunolabeling of the respective transgenic gametocytes with sera from non-immunized mice, rats, or rabbits did not result in any labeling (Figure S9b).

For the HA-tagged PSOP1 and GEVP1, we evaluated the vesicular localization in more detail via super-resolution microscopy. Colabeling experiments, using anti-HA antibodies, revealed overlapping signals of both PSOP1 and GEVP1 with G377, while the two proteins did not co-label with PPLP2 (Figure 6a). No labeling was observed, when gametocytes of the respective PSOP1-HA-*glmS* and GEVP1-HA-*glmS* lines were immunolabeled with serum of non-immunized mice, rats, or rabbits (Figure S10). Colocalization was quantified in IFAs and PCC values were evaluated for each double-labeling experiment. The signal patterns of PSOP1 and GEVP1 overlapped with G377 with PCC values of 0.85 and 0.6, respectively, pointing to a localization of the two proteins in the OBs. In contrast, the signal overlap of the two proteins with PPLP2 resulted in low PCC values of 0.44 and 0.27, respectively (Figure 6b).

Eventually, the fate of PSOP1 during gametocyte activation was determined. Activated gametocytes between 0 and 20 min were immunolabeled with anti-HA antibody to detect PSOP1. The gametocytes were either counterstained by P230 labeling or the OBs were highlighted by G377 immunolabeling (Figure 6c; Figure S11a,b). The

TABLE 1 Selected GEVPs additionally identified by other GEVP proteomics studies. Combined shared hits from Grasso et al. (2020, 2022), Kehrer, Frischknecht, et al. (2016), and Suárez-Cortés et al. (2016).

Short name	GeneID *P. falciparum*	GeneID *P. berghei*	Egress vesicle	SUB2 substrate	Functional category	Loss-of-function phenotype
PSOP12	PF3D7_0513700	PBANKA_1113400	OB	No	Unknown	Unknown
Unknown	PF3D7_0721100	PBANKA_0618600	OB	Yes	Unknown	Unknown
PSOP1	PF3D7_0721700	PBANKA_0619200	OB	No	Unknown	Unknown
PMX	PF3D7_0808200	PBANKA_1222500	OB	Yes	Protein processing, host cell exit	Impaired RBC egress in merozoites (Nasamu et al., 2017)
GAMA	PF3D7_0828800	PBANKA_0701900	Unclear	Yes	Protein adhesion, host cell invasion	Unknown
Falstatin/ ICP	PF3D7_0911900	PBANKA_0813000	OB	Yes	Protein processing, host cell invasion	Impaired sporozoite gliding motility (Boysen & Matuschewski, 2013; Lehmann et al., 2014)
RhopH2	PF3D7_0929400	PBANKA_0830200	Unclear	Yes	Host cell invasion	Unknown
EXP3	PF3D7_1024800	PBANKA_0509000	Unclear	Yes	Protein trafficking	Unknown
Pf11-1	PF3D7_1038400	PBANKA_0300600	OB	No	Host cell exit	Unknown
DPAP1	PF3D7_1116700	PBANKA_0921300	OB	Yes	Protein processing	Unknown
M16	PF3D7_1121800	PBANKA_0926500	Unclear	No	Protein processing	Unknown
PV1	PF3D7_1129100	PBANKA_0919100	OB	Yes	Protein trafficking	Impaired cytoadherence (Batinovic et al., 2017)
SUB2	PF3D7_1136900	PBANKA_0911700	OB	Yes	Host cell invasion, host cell exit	Impaired RBC invasion by merozoites (Collins et al., 2020)
GEXP12	PF3D7_1148700	PBANKA_1226100	OB	Yes	Unknown	Unknown
MDV1	PF3D7_1216500	PBANKA_1432200	OB	Yes	Host cell exit	Impaired gametocyte development and RBC egress (Furuya et al., 2005; Lal et al., 2009; Olivieri et al., 2015)
PPLP2	PF3D7_1216700	PBANKA_1432400	P-EV	No	RBC perforation, host cell exit	Impaired RBCM perforation during gametogenesis (Deligianni et al., 2013; Wirth et al., 2014)
MiGS	PF3D7_1234400	PBANKA_1449000	OB	No	Protein processing, host cell exit	Impaired gametogenesis (Tachibana et al., 2018)
DPAP2	PF3D7_1247800	PBANKA_1460700	OB	No	Protein processing	Unknown
G377	PF3D7_1250100	PBANKA_1463000	OB	No	Host cell exit	Impaired OB biogenesis (de Koning-Ward et al., 2008; Suárez-Cortés et al., 2016)
M1AAP	PF3D7_1311800	PBANKA_1410300	P-EV	Yes	Protein processing	Unknown
P47	PF3D7_1346800	PBANKA_1359700	Unclear	No	Immune evasion, other	Impaired macrogamete fertility
PMIV	PF3D7_1407800	PBANKA_1034400	Unclear	Yes	Protein processing	Reduced erythrocytic replication (Spaccapelo et al., 2010)
PTEX150	PF3D7_1436300	PBANKA_1008500	Unclear	Yes	Protein trafficking	Reduced erythrocytic replication and protein export (Elsworth et al., 2014)
GEST	PF3D7_1449000	PBANKA_1312700	OB	No	Host cell exit	Impaired gametogenesis (Talman et al., 2011)
APP	PF3D7_1454400	PBANKA_1318100	OB	Yes	Protein processing	Unknown

Note: Details can be found in Tables S3 and S4. For geneIDs, see plasmodb.org. SUB2 substrates are according to Collins et al. (2020). OB, osmiophilic body; P-EV, PPLP2-positive egress vesicle; RBC, red blood cell, RBCM, RBC membrane.

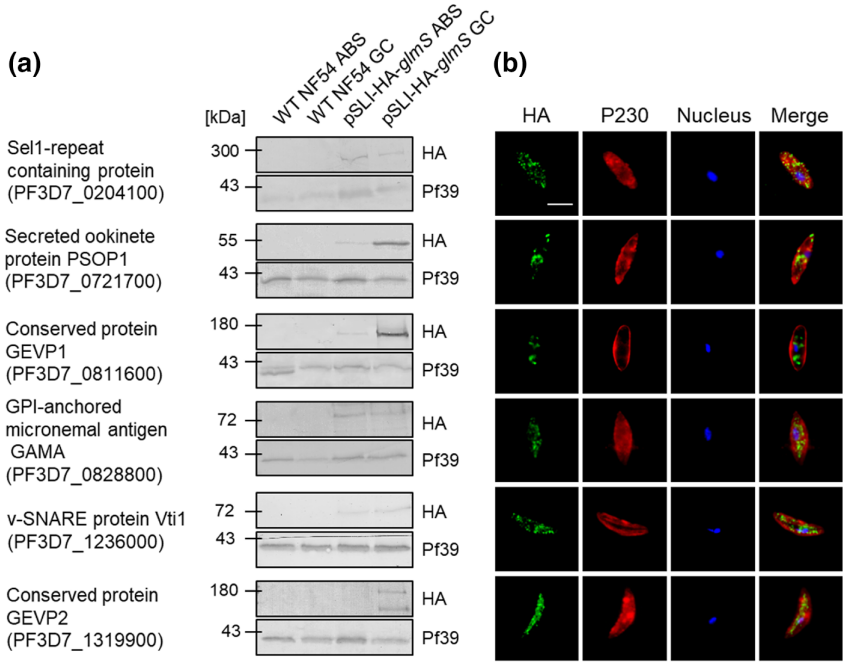

FIGURE 5 Expression and localization of GEVPs in blood stage parasites. Six pSLI-HA-*glmS*-based parasite lines expressing selected GEVPs tagged with HA were generated for expression analysis. (a) Blood stage expression of egress vesicle proteins. Lysates of asexual blood stages (ABS) and gametocytes (GC) of the respective lines were immunoblotted with rat anti-HA antibody to detect Sel1 (271 kDa), PSOP1 (53 kDa), GEVP1 (144 kDa), GAMA (86 kDa) Vti1 (49 kDa) and GEVP2 (179 kDa). ABS and GC lysates of WT NF54 served as negative controls, while immunoblotting with rabbit antibody against the ER protein Pf39 (39 kDa) served as loading control. (b) Vesicular localization of the GEVPs in gametocytes. Gametocytes of the pSLI-HA-*glmS*-based parasite lines were immunolabeled with rat anti-HA antibody (green) to detect the respective HA-tagged GEVP. Gametocytes were counterstained with anti-P230 antisera (red); parasite nuclei were highlighted by Hoechst 33342 nuclear stain (blue). Bar; 5 µm. Cloning strategy and transfection verification are provided in Figure S8. Details on GEVP localization in gametocytes are provided in Figure S9. Results (a, b) are representative of three independent experiments.

IFAs revealed that both PSOP1 and G377 were discharged simultaneously within the first two minutes following activation.

In conclusion, we confirmed the vesicular expression of selected candidates of OBs and P-EVs and in addition demonstrated that PSOP1 is a marker of OBs in *P. falciparum* gametocytes, which is released into the PV lumen immediately following gametocyte activation.

3 | DISCUSSION

The exit of activated gametocytes from the RBC is dependent on the exocytosis of specialized secretory vesicles following the perception of the egress signal. Activation triggers the sequential discharge of OBs needed to rupture the PVM as well as of PPLP2-positive P-EVs that are important for the perforation of the RBCM. The aim of the present study was to characterize the two types of gametocyte-specific egress vesicles in the human malaria species *P. falciparum* by investigating their modes of action upon gametocyte activation and by evaluating their distinct proteomes.

For our analyses, we used marker proteins typical for the two types of egress vesicles; on the one hand, PPLP2 was chosen as a marker for P-EVs, while on the other hand, two marker proteins, that is, G377 and MDV1, served to highlight the OBs. G377 is a well-known component of female OBs (Alano et al., 1995; de Koning-Ward et al., 2008; Olivieri et al., 2015; Severini et al., 1999; Suárez-Cortés et al., 2016); its function, however, is still not fully known. G377-deficient gametocytes have previously been generated by two independent approaches, resulting in different transgenic lines with different loss-of-function phenotypes. In a first approach, de Koning-Ward et al. (2008) demonstrated impaired egress of the G377-deficient gametocytes from RBCs, while the second approach by Suárez-Cortés et al. (2014, 2016) described normal RBC egress, but reduced transmission of G377-deficient parasites. Both studies reported, with reference to exemplary electron micrographs, that gametocytes deficient of G377 lack electron-dense OBs and thus concluded that G377 must be important for OB biogenesis. None of the studies, however, took into consideration that the OBs may still be present, but due to the loss of G377 may be less electron-dense and therefore not well stainable by osmium; hence, a potential link between G377 and OB formation still needs to be proven. In order to also cover male OBs, we included MDV1 as a second marker protein, which has been used for OB-specific BioID–MS analyses before (Kehrer, Frischknecht, et al., 2016). Noteworthy, MDV1 is present in male and female OBs of *P. berghei*, but is additionally present in the PV (Furuya et al., 2005; Lal et al., 2009; Lanfrancotti et al., 2007; Olivieri et al., 2015). In *P. berghei*, MDV1 has been linked to gametogenesis, in particular to PVM rupture, by two independent studies

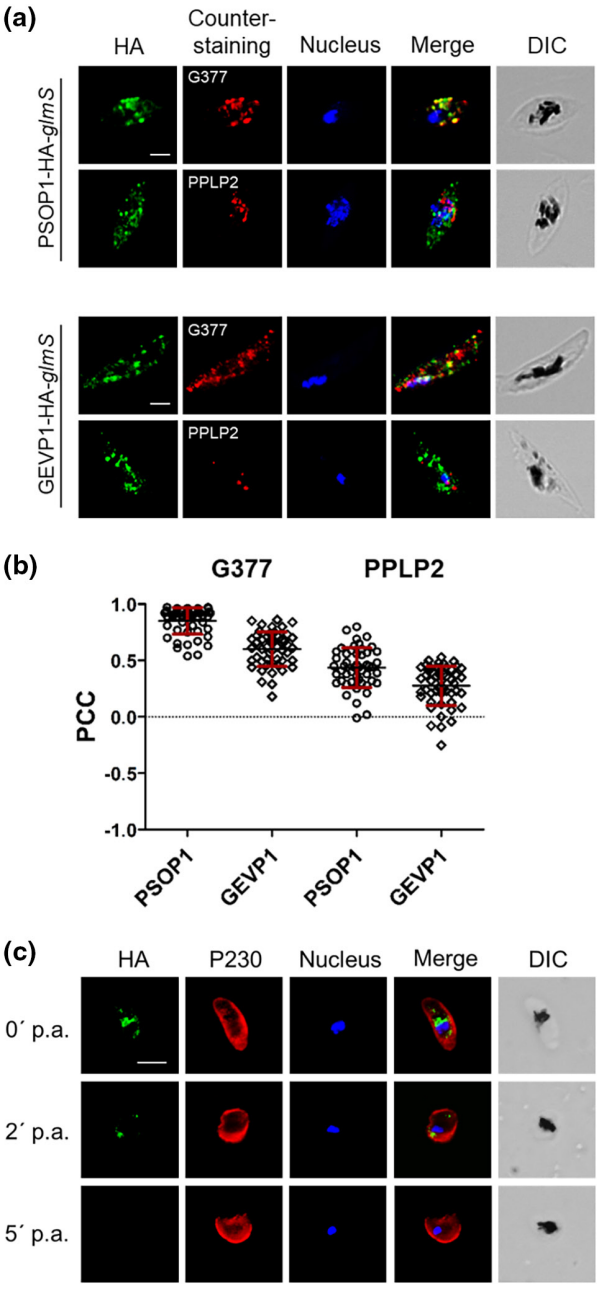

FIGURE 6 Localization and discharge of OB components. (a) Localization of PSOP1 and GEVP1 in OBs. Gametocytes of lines PSOP1-HA-*glmS* and GEVP1-HA-*glmS* were immunolabeled with rat anti-HA antibody (green). OBs and P-EVs were highlighted using rabbit anti-G377 or mouse anti-PPLP2 antisera (red); parasite nuclei were highlighted by Hoechst 33342 nuclear stain (blue). Samples were analyzed via Airyscan super-resolution microscopy. Bar; 2 µm. DIC, differential interference contrast. Corresponding negative controls are provided in Figure S10. (b) Quantification of protein colocalization. The PCC was calculated using Fiji ImageJ2. Immunolabeling of HA-tagged OB proteins was defined as region of interest ($n = 50$). The error bars indicate mean ± SD. (c) PSOP1 discharge following gametocyte activation. Gametocytes of line PSOP1-HA-*glmS* were collected at 0–5 min post-activation (p.a.) and immunolabeled with rat anti-HA antibody to highlight PSOP1 (green). Gametocytes were counterstained by rabbit anti-P230 antisera (red); parasite nuclei were highlighted by Hoechst 33342 nuclear stain (blue). Bar; 5 µm. DIC, differential interference contrast. Further details on PSOP1 discharge are provided in Figure S11. Results (a, c) are representative of three independent experiments.

(Lal et al., 2009; Olivieri et al., 2015); in *P. falciparum*, though, MDV1 was reported to be important for male gametocyte maturation, while a potential function during gametogenesis has not yet been investigated (Furuya et al., 2005). By choosing both G377 and MDV1 for BioID–MS, we were able to cover the range of OB components in the best possible way. While the loss-of-phenotype analyses on G377 and MDV1 are partially contradictory and hence the exact role of the proteins in gametocytes is hitherto unclear, the role of PPLP2 in RBCM perforation and thus RBC exit has been demonstrated in *P. falciparum* and *P. berghei* by three independent studies (Deligianni et al., 2013; Hentzschel et al., 2020; Wirth et al., 2014).

Firstly, we investigated the egress vesicle dynamics in *P. falciparum* gametocytes and demonstrated that OBs and P-EVs are two different types of vesicles with independent modes of exocytosis. We described the consecutive exocytosis of the two vesicle types following gametocyte activation, with only the latter one being dependent on intracellular calcium. These observations are in accord with our previous findings reporting that OBs discharge their content into the PV prior to PVM breakdown at 1 min post-activation, while PPLP2-containing vesicles discharge approximately 6 min later to perforate the RBCM and that PPLP2 release, but not OB exocytosis, can be impaired by calcium chelators (Sologub et al., 2011; Wirth et al., 2014).

In the following, we performed BioID–MS analyses to investigate putative interactors of G377, MDV1, and PPLP2 and identified a total of 143 GEVPs. Among others, we found several previously described mediators of egress, which, in addition to the bait proteins, include for example, Pf11-1, GEST, GEP, MiGS, GEXP02, SUB2, EPF1, and PMX (Andreadaki et al., 2020; Grasso et al., 2020; Kehrer, Frischknecht, et al., 2016; Mbengue et al., 2013; Nasamu et al., 2017; Olivieri et al., 2015; Pace et al., 2019; Pino et al., 2017; Scherf et al., 1992; Suárez-Cortés et al., 2016; Tachibana et al., 2018; Talman et al., 2011; Warncke et al., 2020; reviewed in Bennink & Pradel, 2021; Kuehn & Pradel, 2010; Pradel, 2007). Noteworthy, the majority of the identified GEVPs could be assigned to the OBs, pointing to a major role of these vesicles in egress from the enveloping RBC.

In addition to egress factors, we identified novel GEVPs previously assigned to other functions and lifecycle stages, for example, merozoite proteins like RhopH2, MaTrA, MSP8, and P38, all of which are known to be involved in RBC invasion (Black et al., 2005; Cowman et al., 2017; Curtidor et al., 2004; Hinds et al., 2009; Molina-Franky et al., 2022; Ntumngia et al., 2004; Sanders et al., 2005; Vincensini et al., 2008), or the PSOP members PSOP1, PSOP12, PSOP13, PSOP17, and GAMA (the ortholog of *P. berghei* PSOP9) originally described in the ookinete micronemes and assigned to mosquito midgut penetration (Ecker et al., 2008; Tachibana et al., 2021). The fact that the here identified egressome includes proteins important for merozoite invasion as well as ookinete proteins assigned to

midgut extravasation suggests that these proteins may have multiple functions related to host cell membrane modification in different lifecycle stages. Since a considerable proportion of the GEVPs are proteins originally assigned to merozoites and since some of them have previously been reported to be directly involved in merozoite egress, for example, EPF1 and PMX (see above), merozoites and gametocytes appear to share a basic repertoire of egress-related proteins. Unfortunately, to date no exoneme-specific proteome has been identified, hence, comparative analyses between GEVPs and exoneme-resident proteins are not yet possible.

We also identified various proteases, for example, SUB2, DPAP1, DPAP2, M1AAP, M16, as well as PMI, PMIII, PMX, the majority of which were so far linked to hemoglobin processing (reviewed in, e.g., Arisue et al., 2020; Goldberg, 2005; Nasamu et al., 2020; Rosenthal, 2002; Siqueira-Neto et al., 2018; Trenholme et al., 2010). Importantly, approximately one third of the identified GEVPs were recently shown to be putative SUB2 substrates (Collins et al., 2020). SUB2 is a sheddase originally identified in merozoites that is discharged from micronemes to process merozoite surface proteins like MSP1 during the invasion of RBCs. Because SUB2 was identified by us and others as a putative OB-resident protein and due to the fact that a high proportion of the identified GEVPs are known SUB2 substrates, we hypothesize a role of SUB2 in processing select GEVPs prior to or after OB exocytosis.

Furthermore, a high number of GEVPs was previously associated to the Maurer's clefts, like the gametocyte exported protein family members GEXP02, GEXP17, GEXP12, GEXP21, and GEXP22, further EPF1, PTP5, ETRAMP10.2, MSRP5, and PV1 as well as various PHIST proteins and unnamed exported proteins. These proteins may function in remodeling the erythrocyte cytoskeleton as a preceding step of RBCM rupture.

The identification of PPLP2-specific interactors proved difficult, even after repetition of the BioID analysis using another independent duplicate. The majority of PPLP2 interactors can be assigned to vesicle biogenesis, particularly transmembrane transporters. To be highlighted is the interaction of PPLP2 with the v-SNARE protein Vti1, which is one of three identified *P. falciparum* orthologs of eukaryotic Vti1 (Aurrecoechea et al., 2009; Ayong et al., 2007). Indeed, *in silico* and transcript and protein expression analyses confirmed that many factors of the vesicle trafficking and fusion machinery, including SNAREs and associated proteins, are conserved in *P. falciparum* and expressed in gametocytes (reviewed in Bennink & Pradel, 2021). The role of these molecules in the dynamics of egress vesicles, however, is yet unknown and needs to be investigated in more detail.

Several of the identified candidates were interactors shared by PPLP2 with G377 and/or MDV1. The majority of these proteins belong to the LCCL-domain protein-based multi-adhesion domain protein complex, including CCp1, CCp2, CCp3, CCp5, and FNPA as well as the P48/45 and P230. It has previously been shown that the components of this multi-adhesion domain protein complex are expressed throughout gametocyte maturation and localize in the PV, where the complex is anchored in the GPM via P48/45 (Pradel et al., 2004; Scholz et al., 2008; Simon et al., 2009, 2016; reviewed in Kuehn et al., 2010; Pradel, 2007). IFAs confirmed the presence of CCp2 in vesicles and the PV and showed that CCp2 does neither colabel with G377 nor PPLP2. These results suggest that the components of the multi-adhesion domain protein complex have met the biotin ligase-tagged bait proteins during endomembrane trafficking. The encounter of secretory proteins during endomembrane trafficking would also explain why PPLP2 was previously identified as an interactor of MDV1 (Kehrer, Frischknecht, et al., 2016).

In a last step of our study, we selected six known and yet uncharacterized components of the egress vesicle interactomes, including the novel v-SNARE Vti1, and verified their vesicular localization. In addition, we confirmed an OB-specific localization of PSOP1 and GEVP1. The verification of PSOP1 as an OB-resident protein strengthens our hypothesis that PSOP proteins have additional functions distinct from ookinete biology. In this context, a recent study identified naturally acquired antibodies against PSOP1 in blood samples of various malaria cohorts, verifying the presence of the protein in gametocytes (Muthui et al., 2021). Similarly, PSOP12, another egress molecule identified in this study that is a member of the 6-cys family, was demonstrated to be expressed in gametocytes in addition to ookinetes (Annoura et al., 2014; Sala et al., 2015; Wass et al., 2012). The expression of such PSOP members from gametocyte maturation until ookinete development makes them promising candidates for transmission blocking vaccines (Sala et al., 2015).

In conclusion, we here demonstrated the presence of two different types of egress vesicles, the OBs and P-EVs, with important functions during RBC exit by activated gametocytes. We further verified the existence of various OB components in *P. falciparum*, which were previously identified in *P. berghei*. In addition, we identified novel components of the two egress vesicle types, including Maurer's cleft-associated proteins, proteases, transmembrane transporters, and vesicle trafficking proteins, but also various yet unknown proteins. Because the OB proteome contains the vast majority of the GEVPs, we conclude that these vesicles play a major role in RBC egress. The fact that most of the identified GEVPs have orthologs in *P. berghei* further points to a conserved egress mechanism in malaria parasites. Follow-up studies will need to verify the role of GEVPs in gametogenesis in order to shed more light on the molecular machinery of the inside-out egress of gametocytes.

4 | EXPERIMENTAL PROCEDURE

4.1 | Gene identifiers

Aldolase (PF3D7_1444800), CCp2 (PF3D7_1455800); G377 (PF3D7_1250100);GAMA(PF3D7_0828800)GEVP1(PF3D7_0811600); GEVP2 (PF3D7_1319900); MDV1 (PF3D7_1216500); Pf39 (PF3D7_1108600); Pf92 (PF3D7_1364100); P230 (PF3D7_0209000); Pfs16 (PF3D7_0406200); PPLP2 (PF3D7_1216700), PSOP1 (PF3D7_0721700); Sel1 (PF3D7_0204100), Vti1 (PF3D7_1236000).

4.2 | Bioinformatics

Colocalization of G377, MDV1, and PPLP2 in IFAs was evaluated via Pearson's correlation coefficient (PCC) using Fiji ImageJ2 (Schindelin et al., 2012). Prediction of the transmembrane domains and intra−/extracellular regions of the putative interaction partners was performed using DeepTMHMM (Hallgren et al., 2022); further signal peptide prediction was performed using the SignalP versions 4.1 with sensitive D-cutoff and 5.0 (Almagro Armenteros et al., 2019; Petersen et al., 2011). Subcellular localization regarding potential ER localization was predicted using DeepLoc 2.0, ER-retention signals were identified based on a bioinformatic analysis of Külzer et al. (2009) and Thumuluri et al. (2022). Predictions of gene expression and protein function were made using the database PlasmoDB (http://plasmoDB.org; Aurrecoechea et al., 2009); the peak transcript expression of candidate genes was analyzed using table "Transcriptomes of 7 sexual and asexual life stages" (López-Barragán et al., 2011) and sex specificity was predicted using table "Gametocyte Transcriptomes" (Lasonder et al., 2016) of the PlasmoDB database. A sex specificity was considered, when the transcript per million (TPM) ratio was ≥3. Data mining in the context of gene disruptibility and possible loss-of-function mutant phenotypes was performed using PhenoPlasm (http://phenoplasm.org/; Sanderson & Rayner, 2017), the USF PiggyBac Screen (Zhang et al., 2018), PlasmoGEM (https://plasmogem.umu.se/pbgem/; Schwach et al., 2015), and RMgmDB (https://www.pberghei.eu/index.php; Khan et al., 2013). The GO enrichment analysis was performed using the PlasmoDB database with a *p*-value cutoff of 0.05. A network analysis was conducted using the STRING database (version 11.0) (Szklarczyk et al., 2019), using default settings, including text mining options and a confidence of 0.009.

4.3 | Antibodies

The following antisera were used: rabbit polyclonal antisera against G377 (Severini et al., 1999; kindly provided by Pietro Alano, Istituto Superiore di Sanità, Rome, Italy), CCp2 (Roling et al., 2022; Simon et al., 2009, 2016), Pf39 (Simon et al., 2009), Pf92 (Musabyimana et al., 2022) P230 (Simon et al., 2009, 2016), and Pfs16 (kindly provided by Kim Williamson, Uniformed Services University of the Health Sciences, Bethesda, US); mouse polyclonal antisera against Pf92 (Musabyimana et al., 2022); PPLP2 (Wirth et al., 2014), CCp2 (Pradel et al., 2004), P230 (Williamson et al., 1995), or Pfs16 (kindly provided by Kim Williamson, Uniformed Services University of the Health Sciences, Bethesda, US; Sologub et al., 2011); rat polyclonal antisera against MDV1 (kindly provided by Pietro Alano, Istituto Superiore di Sanità, Rome, Italy), monoclonal mouse anti-GFP antibody (Roche; Basel, CH). monoclonal rat anti-HA antibody (Roche; Basel, CH), monoclonal mouse anti-human spectrin alpha-1 antibody 17C7 (Invitrogen Molecular Probes; Eugene, US), and polyclonal rabbit anti-spectrin alpha 1 antibody (Invitrogen Molecular Probes; Eugene, US).

4.4 | Parasite culture

In this study, *P. falciparum* strain NF54 (WT NF54) was used. The WT NF54 and all generated mutant parasite lines were cultivated *in vitro* in human blood group A+ erythrocytes as previously described (Ifediba & Vanderberg, 1981). Asexual blood stages and gametocytes were maintained in RPMI1640/HEPES medium (Gibco; Thermo Fisher Scientific; Waltham, US) supplemented with 10% (v/v) heat inactivated human A+ serum, 50 μg/mL hypoxanthine (Sigma-Aldrich; Taufkirchen, DE) and 10 μg/mL gentamicin (Gibco; Thermo Fisher Scientific; Waltham, US). For cultivation of the mutant parasite lines, the selection drug WR99210 (Jacobus Pharmaceutical Company; Princeton, US) was added in final concentrations of 2.5 nM or 4.0 nM. All cultures were kept at 37°C in an atmosphere of 5% O_2 and 5% CO_2 in N_2. Gametocytes were enriched via Percoll (Cytiva; Washington DC, US) gradient centrifugation as described previously (Kariuki et al., 1998). Gametogenesis was induced by adding xanthurenic acid in a final concentration of 100 μM dissolved in 1% (v/v) 0.5 M NH_4OH/ddH_2O and incubation for 15 min at room temperature (RT). To analyze the role of intracellular calcium during exocytosis, the cultures were treated with 25 μM BAPTA–AM (Thermo Fisher Scientific; Waltham, US) for 15 min at 37°C prior to activation. Erythrocyte concentrate and serum from humans were procured from the Department of Transfusion Medicine (RWTH University Hospital Aachen, Germany). All work with human blood was approved by the RWTH University Hospital Aachen Ethics commission, the donors remained anonymous and serum samples were pooled.

4.5 | Generation of parasite lines to be used in BioID

Plasmid pSLI-TurboID-GFP (pSL1423; Addgene #194904) was created to serve as a base plasmid for the fusion of TurboID with the C-terminus of the respective protein of interest by modifying the previously described pSLI–TGD plasmid (Addgene #85791, Birnbaum et al., 2017) via inserting a recodonized version of TurboID ("V4") and a portion of GFPmut2 between the existing NotI and HpaI sites. For the generation of the MDV1- and G377-TurboID-GFP parasite lines, a gene fragment homologous to the 3′-region of the gene was amplified via PCR using the respective primers (for primer sequences, see Table S6). Ligation of insert and vector backbone was mediated by NotI and SpeI restriction sites. A WT NF54 culture with at least 5% ring stages was transfected with 100 μg plasmid DNA in transfection buffer via electroporation (310 V, 950 μF, 12 ms; Bio-Rad gene-pulser Xcell) as described (e.g., Ngwa et al., 2017; Wirth et al., 2014). At 6 h post-transfection, WR99210 was added in a final concentration of 4 nM. A mock control was electroporated using transfection buffer without the addition of plasmid DNA and was cultured in medium with and without WR99210. After approximately 3–5 weeks, WR-resistant parasites appeared in the cultures. To remove WT NF54 parasites from the culture, these were treated with 800 μg/mL neomycin (G418

disulfate salt; Sigma-Aldrich; Taufkirchen, DE) daily for a maximum of 7 days. To verify successful integration into the respective gene locus, genomic DNA (gDNA) was isolated from the transgenic parasite lines, using the NucleoSpin Blood Kit (Macherey-Nagel; Dueren, DE) following the manufacturer's protocol and used as template in diagnostic PCR. The following primers were used to confirm vector integration: 5′Int MDV1/G377-TurboID, 3′Int MDV/G377-TurboID, pARL-HA-*glmS* FP, pGREP RP (for primer sequences, see Table S6). The PPLP2-GFP-BirA parasite line was generated by using vector pARL-*pffnpa*-GFP-BirA (Musabyimana et al., 2022). The full-length gene was amplified via PCR using the respective primers (for primer sequences, see Table S6). Ligation of insert and vector backbone was mediated by KpnI and AvrII restriction sites. Transfection of the construct was carried out as described above. Episomal presence of the construct was checked by using the following primers: PPLP2-BirA-KpnI-FP and pGREP RP (for primer sequences, see Table S6).

4.6 | Generation of pSLI-HA-*glmS* parasite lines

The HA-*glmS*-tagged parasite lines were generated via single-crossover homologous recombination, using vector pSLI-HA-*glmS* (Musabyimana et al., 2022; kindly provided by Dr. Ron Dzikowski, The Hebrew University of Jerusalem, Israel). A gene fragment homologous to the 3′-region of the gene was amplified via PCR using the respective primers (for primer sequences, see Table S6). The ligation of insert and vector backbone was mediated by NotI and XmaI restriction sites. The transfection and selection procedures were performed as described above, but WR99210 was added in a final concentration of 2.5 nM. The following primers were used to confirm vector integration: 5′-Integration Construct pSLI-*glmS*, 3′-Integration Construct pSLI-*glmS*, pARL-HA-*glmS* FP, pSLI-HA-*glmS* RP (for primer sequences, see Table S6).

4.7 | Western blot analysis

Asexual blood stage parasites of WT NF54, lines MDV1- and G377-TurboID-GFP, line PPLP2-GFP-BirA, and the HA-*glmS*-tagged parasite lines were harvested from mixed cultures. For erythrocyte lysis, parasites were incubated for 10 min in 0.05% (w/v) saponin/PBS. Gametocytes were enriched by Percoll purification as described above. Pelleted parasites were resuspended in lysis buffer (150 mM NaCl, 0.1% (v/v) Triton X-100, 0.5% (w/v) sodium deoxycholate, 0.1% (w/v) SDS, 50 mM Tris–HCl, pH 8.0) supplemented with protease inhibitor cocktail (PIC, Roche; Basel, CH). A 5× SDS loading buffer with 25 mM dithiothreitol was added to the lysates, followed by heat-denaturation for 10 min at 95°C. Lysates were separated via SDS–PAGE and transferred to a nitrocellulose membrane. Non-specific binding sites were blocked by incubation with 5% (w/v) skim milk and 1% (w/v) BSA in Tris-buffered saline (pH 7.5) for 1 h at 4°C. For immunodetection, membranes were incubated overnight at 4°C with monoclonal mouse anti-GFP antibody (Roche; Basel, CH; dilution 1:500) or monoclonal rat anti-HA antibody (Roche; Basel, CH; dilution 1:200) and polyclonal rabbit anti-Pf39 antisera (dilution 1:10,000) in 3% (w/v) skim milk/TBS. The membranes were washed 3x each with 3% (w/v) skim milk/TBS and 3% (w/v) skim milk/0.1% (v/v) Tween/TBS and then incubated for 1 h at RT with goat anti-mouse, anti-rabbit or anti-rat alkaline phosphatase-conjugated secondary antibodies (dilution 1:10,000, Sigma-Aldrich; Taufkirchen, DE) in 3% (w/v) skim milk/TBS. The membranes were developed in a NBT/BCIP solution (nitroblue tetrazolium chloride/5-bromo-4-chloro-3-indoxyl phosphate; Roche; Basel, CH) for up to 20 min at RT. For the detection of biotinylated proteins, the blocking step was performed overnight at 4°C in 5% (w/v) skim milk/TBS and the membrane was washed 5× with 1× TBS before incubation with streptavidin-conjugated alkaline phosphatase (dilution 1:1000, Sigma-Aldrich; Taufkirchen, DE) in 5% (w/v) BSA/TBS for 1 h at RT.

4.8 | Indirect immunofluorescence assay

Asexual blood stage parasites and gametocytes of WT NF54, lines MDV1-TurboID-GFP, G377-TurboID-GFP, and PPLP2-GFP-BirA, and the HA-*glmS*-based parasite lines were coated on diagnostic slides (Epredia; Thermo Fisher Scientific; Waltham, US) and air-dried. Fixation of the cells was performed with 40 µL of 4% (w/v) paraformaldehyde (pH 7.2) for 10 min at RT, followed by membrane permeabilization with 30 µL of 0.1% (v/v) Triton X-100/125 mM glycerol for another 10 min at RT. Non-specific binding sites were blocked by incubation with 3% (w/v) BSA/PBS for 30 min. The primary antibodies were diluted in 3% (w/v) BSA/PBS and were added to the slide for 2 h incubation at 37°C. The slides were washed 3× with PBS and incubated with the secondary antibody for 1 h at 37°C. Following 2× washing with PBS, the incubation with the second primary antibody and the corresponding visualization with the second secondary antibody were carried out as described above. The nuclei were stained with Hoechst 33342 staining solution for 2 min at RT (1:5000 in 1× PBS). The cells were mounted with anti-fading solution (Citifluor Limited; London, UK), covered with a coverslip and sealed airtight with nail polish. The parasites were visualized by either conventional fluorescence microscopy using a Leica DM5500 B (Leica; Wetzlar, DE) or by confocal microscopy using Zeiss LSM880 Airyscan super-resolution microscope (Carl Zeiss; Jena, DE) fitted with an Airyscan detector and a Plan-Apochromat ×63 (NA 1.4) M27 oil objective. During confocal microscopy, the images were acquired sequentially with a pixel resolution of 0.02 µm in four channels as follows: channel 1 = 405 nm laser, channel 2 = 488 nm laser, channel 3 = 561 nm laser, channel 4 = differential interference contrast (DIC). Antibodies were diluted as follows: rat anti-MDV1 (1:1000), rabbit anti-G377 (1:1000), mouse anti-PPLP2 (1:50), mouse anti-GFP (1:500), rat anti-HA (1:100), anti-CCp2 (mouse, 1:50; rabbit, 1:500), mouse and rabbit anti-Pf92 (1:500) mouse and rabbit anti-P230 (1:400), mouse and rabbit anti-Pfs16 (1:200); mouse and rabbit anti-spectrin (1:500), and anti-mouse Alexa Fluor 488, anti-rabbit Alexa Fluor 488, anti-rat Alexa Fluor

488, anti-mouse Alexa Fluor 594, anti-rabbit Alexa Fluor 594, anti-mouse Alexa Fluor 555 and anti-rabbit Alexa Fluor 555 (1:1000; used for LSM880 microscopy; all fluorophores from Invitrogen Molecular Probes; Eugene, US, or Sigma-Aldrich; Taufkirchen, DE); further Alexa Fluor 594 streptavidin (1:500; Invitrogen Molecular Probes; Eugene, US) was used.

4.9 | Statistical analysis

Data are expressed as mean ± SD. Statistical differences were determined using One-Way ANOVA with post-hoc Bonferroni Multiple Comparison test. *p*-values <0.05 were considered statistically significant. Significances were calculated using GraphPad Prism 5 and are defined as follows: $^{*}p < 0.05$; $^{**}p < 0.01$; $^{***}p < 0.001$.

4.10 | Affinity purification of biotinylated proteins

The lines MDV1-TurboID-GFP, G377-TurboID-GFP and PPLP2-GFP-BirA were used for BioID-MS analysis, following a protocol by Roux et al. (2018). WT NF54 cultures were used for control. Biotinylation was induced by treatment of the corresponding gametocyte cultures with 50 μM biotin for 15 min (TurboID) or 20 h (BioID) at 37°C. Gametocytes were washed in RPMI incomplete medium, enriched via Percoll gradient centrifugation, and resuspended in 100 μL binding buffer (Tris-buffered saline containing 1% (v/v) Triton X-100 and protease inhibitor). The sample was sonicated on ice (2 × 60 pulses at 30% duty cycle) and another 100 μL of ice-cold binding buffer was added. After a second session of sonification, cell debris was pelleted by centrifugation (5 min, 16,000× *g*, 4°C). The supernatant was mixed with pre-equilibrated Cytiva Streptavidin Mag Sepharose Magnet-Beads (Cytiva; Washington DC, US) in a low-binding reaction tube. Incubation was performed with slow end-over-end mixing over night at 4°C. The beads were washed 6× with 500 μL washing buffer (3×: RIPA buffer containing 0.03% (w/v) SDS, followed by 3× 25 mM Tris buffer, pH 7.5) and were resuspended in 100 μL elution buffer (1% (w/v) SDS/5 mM biotin in Tris buffer (pH 7.5)), followed by an incubation for 5 min at 95°C. The supernatant was transferred into a new reaction tube and stored at 4°C. For each culture, three independent samples were collected; two additional independent samples for line PPLP2-GFP-BirA line were included.

4.11 | Proteolytic digestion

Samples were processed by single-pot solid-phase-enhanced sample preparation (SP3) as described before (Hughes et al., 2014; Sielaff et al., 2017). Eluted proteins were reduced and alkylated, using DTT and iodoacetamide (IAA), respectively. Afterward, 2 μL of carboxylate-modified paramagnetic beads (Sera-Mag Speed Beads, GE Healthcare; Chicago, US; 0.5 μg solids/μL in water as described by Hughes et al., 2014) were added to the samples. After adding acetonitrile to a final concentration of 70% (v/v), samples were allowed to settle at RT for 20 min. Subsequently, beads were washed twice with 70% (v/v) ethanol in water and once with acetonitrile. The beads were resuspended in 50 mM NH_4HCO_3 supplemented with trypsin (Mass Spectrometry Grade, Promega; Madison, US) at an enzyme-to-protein ratio of 1:25 (w/w) and incubated overnight at 37°C. After overnight digestion, acetonitrile was added to the samples to reach a final concentration of 95% (v/v) followed by incubation at RT for 20 min. To increase the yield, supernatants derived from this initial peptide-binding step were additionally subjected to the SP3 peptide purification procedure (Sielaff et al., 2017). Each sample was washed with acetonitrile. To recover bound peptides, paramagnetic beads from the original sample and corresponding supernatants were pooled in 2% (v/v) dimethyl sulfoxide (DMSO) in water and sonicated for 1 min. After 2 min of centrifugation at 14,000× *g* and 4°C, supernatants containing tryptic peptides were transferred into a glass vial for MS analysis and acidified with 0.1% (v/v) formic acid.

4.12 | Liquid chromatography-mass spectrometry (LC–MS) analysis

Tryptic peptides were separated using an Ultimate 3000 RSLCnano LC system (Thermo Fisher Scientific; Waltham, US) equipped with a PEPMAP100 C18 5 μm 0.3 × 5 mm trap (Thermo Fisher Scientific; Waltham, US) and an HSS-T3 C18 1.8 μm, 75 μm × 250 mm analytical reversed-phase column (Waters Corporation; Milford, US). Mobile phase A was water containing 0.1% (v/v) formic acid and 3% (v/v) DMSO. Peptides were separated by running a gradient of 2%–35% mobile phase B (0.1% (v/v) formic acid, 3% (v/v) DMSO in ACN) over 40 min at a flow rate of 300 nL/min. Total analysis time was 60 min including wash and column re-equilibration steps. Column temperature was set to 55°C. Mass spectrometric analysis of eluting peptides was conducted on an Orbitrap Exploris 480 (Thermo Fisher Scientific; Waltham, US) instrument platform. Spray voltage was set to 1.8 kV, the funnel RF level to 40, and heated capillary temperature was at 275°C. Data were acquired in data-dependent acquisition (DDA) mode targeting the 10 most abundant peptides for fragmentation (Top10). Full MS resolution was set to 120,000 at *m/z* 200 and full MS automated gain control (AGC) target to 300% with a maximum injection time of 50 ms. Mass range was set to *m/z* 350–1500. For MS2 scans, the collection of isolated peptide precursors was limited by an ion target of 1×10^5 (AGC tar-get value of 100%) and maximum injection times of 25 ms. Fragment ion spectra were acquired at a resolution of 15,000 at *m/z* 200. Intensity threshold was kept at 1E4. Isolation window width of the quadrupole was set to 1.6 *m/z* and normalized collision energy was fixed at 30%. All the data were acquired in profile mode using positive polarity. Each sample was analyzed in three technical replicates.

4.13 | Data analysis and label-free quantification

DDA raw data acquired with the Exploris 480 were processed with MaxQuant (version 2.0.1; Cox & Mann, 2008; Cox et al., 2014), using

the standard settings and label-free quantification (LFQ) enabled for each parameter group, that is, control and affinity-purified samples (LFQ min ratio count 2, stabilize large LFQ ratios disabled, match-between-runs). Data were searched against the forward and reverse sequences of the *P. falciparum* proteome (UniProtKB/TrEMBL, 5445 entries, UP000001450, released April 2020) and a list of common contaminants. For peptide identification, trypsin was set as protease allowing two missed cleavages. Carbamidomethylation was set as fixed and oxidation of methionine as well as acetylation of protein N-termini as variable modifications. Only peptides with a minimum length of 7 amino acids were considered. Peptide and protein false discovery rates (FDRs) were set to 1%. In addition, proteins had to be identified by at least two peptides. Statistical analysis of the data was conducted using Student's *t*-test, which was corrected by the Benjamini-Hochberg (BH) method for multiple hypothesis testing (FDR of 0.01). In addition, proteins in the affinity-enriched samples had to be identified in all three biological replicates and show at least a two-fold enrichment compared to the controls. The datasets of protein hits were further edited by verification of the gene IDs and gene names via the PlasmoDB database (www.plasmodb.org; Aurrecoechea et al., 2009). PlasmoDB gene IDs were extracted from the fasta headers provided by mass spectrometry and verified manually. Once an initial list of significantly enriched proteins had been established, two curation steps were performed: First, proteins without a putative signal peptide and/or transmembrane domains and those with C-terminal ER retention signals were excluded (using programmes DeepTMHMM for transmembrane domain prediction, SignalP version 4.1 and 5.0 for signal peptide prediction, and DeepLoc 2.0 as well as a bioinformatic analysis of Külzer et al. (2009) for ER retention signal prediction as described above). Second, proteins with defined known functions not related to OBs or P-EVs as indicated at PlasmoDB were removed. In addition, the significantly enriched proteins were compared to those previously identified by us as interactors of plasmodial intracellular enzyme SAMS (Musabyimana et al., 2022) and no matches were found.

AUTHOR CONTRIBUTIONS

Juliane Sassmannshausen: Writing – original draft; investigation; methodology; visualization; formal analysis; software. **Sandra Bennink:** Conceptualization; investigation; methodology; validation; formal analysis; software; project administration. **Ute Distler:** Investigation; software; methodology; data curation. **Juliane Küchenhoff:** Methodology; investigation. **Allen M. Minns:** Methodology; resources. **Scott E. Lindner:** Methodology; resources. **Paul-Christian Burda:** Methodology; validation; visualization. **Stefan Tenzer:** Resources; data curation; software; supervision; methodology; funding acquisition. **Tim W. Gilberger:** Conceptualization; resources; supervision; data curation; funding acquisition. **Gabriele Pradel:** Writing – original draft; funding acquisition; validation; formal analysis; project administration; data curation; supervision; resources.

ACKNOWLEDGMENTS

The authors acknowledge funding by the Deutsche Forschungsgemeinschaft (project grant PR905/15-1; DFG priority programme SPP 2225 grants PR905/19-1 to GP, GI312/11-1 to TWG and TE599/9-1 to ST). The authors thank Pietro Alano (Istituto Superiore di Sanità Rome) for providing antisera against G377 and MDV1 and Ron Dzikowski (The Hebrew University of Jerusalem) for providing vector pSLI-HA-*glmS*. The authors further gratefully acknowledge the microscopy support from the Advanced Light and Fluorescence Microscopy (ALFM) facility at the Centre for Structural Systems Biology (CSSB). Open Access funding enabled and organized by Projekt DEAL.

DATA AVAILABILITY STATEMENT

The mass spectrometry proteomics data have been deposited to the ProteomeXchange Consortium (http://proteomecentral.proteomexchange.org) via the jPOSTrepo partner repository (Okuda et al., 2017; Vizcaíno et al., 2013) with the dataset identifiers PXD039679 (ProteomeXchange) and JPST002011 (jPOSTrepo).

ETHICS STATEMENT

Erythrocyte concentrate and serum from humans were procured from the Department of Transfusion Medicine, RWTH University Hospital Aachen, Germany. Donor sera and blood samples were pooled and the donors were kept anonymous. The work with human blood was approved by the Ethics commission of RWTH University Hospital Aachen (EK 007/13). Antibodies used in this study were purchased commercially or have previously been published.

ORCID

Paul-Christian Burda https://orcid.org/0000-0003-0461-4352
Gabriele Pradel https://orcid.org/0000-0003-2264-5558

REFERENCES

Alano, P., Read, D., Bruce, M., Aikawa, M., Kaido, T., Tegoshi, T. et al. (1995) COS cell expression cloning of Pfg377, a *Plasmodium falciparum* gametocyte antigen associated with osmiophilic bodies. *Molecular and Biochemical Parasitology*, *74*(2), 143–156. Available from: https://doi.org/10.1016/0166-6851(95)02491-3

Almagro Armenteros, J.J., Tsirigos, K.D., Sønderby, C.K., Petersen, T.N., Winther, O., Brunak, S. et al. (2019) SignalP 5.0 improves signal peptide predictions using deep neural networks. *Nature Biotechnology*, *37*. *4*, 420–423. Available from: https://doi.org/10.1038/s41587-019-0036-z

Andreadaki, M., Hanssen, E., Deligianni, E., Claudet, C., Wengelnik, K., Mollard, V. et al. (2018) Sequential membrane rupture and vesiculation during *Plasmodium berghei* gametocyte egress from the red blood cell. *Scientific Reports*, *8*(1), 3543. Available from: https://doi.org/10.1038/s41598-018-21801-3

Andreadaki, M., Pace, T., Grasso, F., Siden-Kiamos, I., Mochi, S., Picci, L. et al. (2020) *Plasmodium berghei* gamete egress protein is required for fertility of both genders. *MicrobiologyOpen*, *9*(7), e1038. Available from: https://doi.org/10.1002/mbo3.1038

Annoura, T., van Schaijk, B.C.L., Ploemen, I.H.J., Sajid, M., Lin, J., Vos, M.W. et al. (2014) Two *Plasmodium* 6-Cys family-related proteins have distinct and critical roles in liver-stage development. *FASEB Journal*, *28*(5), 2158–2170. Available from: https://doi.org/10.1096/fj.13-241570

Arastu-Kapur, S., Ponder, E.L., Fonović, U.P., Yeoh, S., Yuan, F., Fonović, M. et al. (2008) Identification of proteases that regulate erythrocyte rupture by the malaria parasite *Plasmodium falciparum*. *Nature Chemical Biology*, *4*(3), 203–213. Available from: https://doi.org/10.1038/nchembio.70

Arisue, N., Palacpac, N.M.Q., Tougan, T. & Horii, T. (2020) Characteristic features of the SERA multigene family in the malaria parasite. *Parasites & Vectors*, *13*(1), 170. Available from: https://doi.org/10.1186/s13071-020-04044-y

Arumugam, T.U., Takeo, S., Yamasaki, T., Thonkukiatkul, A., Miura, K., Otsuki, H. et al. (2011) Discovery of GAMA, a *Plasmodium falciparum* merozoite micronemal protein, as a novel blood-stage vaccine candidate antigen. *Infection and Immunity*, *79*(11), 4523–4532. Available from: https://doi.org/10.1128/IAI.05412-11

Aurrecoechea, C., Brestelli, J., Brunk, B.P., Dommer, J., Fischer, S., Gajria, B. et al. (2009) PlasmoDB: a functional genomic database for malaria parasites. *Nucleic Acids Research*, *37*, D539–D543. Available from: https://doi.org/10.1093/nar/gkn814

Ayong, L., Pagnotti, G., Tobon, A.B. & Chakrabarti, D. (2007) Identification of *Plasmodium falciparum* family of SNAREs. *Molecular and Biochemical Parasitology*, *152*(2), 113–122. Available from: https://doi.org/10.1016/j.molbiopara.2006.12.007

Baldi, D.L., Andrews, K.T., Waller, R.F., Roos, D.S., Howard, R.F., Crabb, B.S. et al. (2000) RAP1 controls rhoptry targeting of RAP2 in the malaria parasite *Plasmodium falciparum*. *The EMBO Journal*, *19*(11), 2435–2443. Available from: https://doi.org/10.1093/emboj/19.11.2435

Banerjee, R., Liu, J., Beatty, W., Pelosof, L., Klemba, M. & Goldberg, D.E. (2002) Four plasmepsins are active in the *Plasmodium falciparum* food vacuole, including a protease with an active-site histidine. *Proceedings of the National Academy of Sciences of the United States of America*, *99*(2), 990–995. Available from: https://doi.org/10.1073/pnas.022630099

Bargieri, D.Y., Thiberge, S., Tay, C.L., Carey, A.F., Rantz, A., Hischen, F. et al. (2016) *Plasmodium* merozoite TRAP family protein is essential for vacuole membrane disruption and gamete egress from erythrocytes. *Cell Host & Microbe*, *20*(5), 618–630. Available from: https://doi.org/10.1016/j.chom.2016.10.015

Batinovic, S., McHugh, E., Chisholm, S.A., Matthews, K., Liu, B., Dumont, L. et al. (2017) An exported protein-interacting complex involved in the trafficking of virulence determinants in *Plasmodium*-infected erythrocytes. *Nature Communications*, *8*, 16044. Available from: https://doi.org/10.1038/ncomms16044

Bennink, S., Kiesow, M.J. & Pradel, G. (2016) The development of malaria parasites in the mosquito midgut. *Cellular Microbiology*, *18*(7), 905–918. Available from: https://doi.org/10.1111/cmi.12604

Bennink, S. & Pradel, G. (2021) Vesicle dynamics during the egress of malaria gametocytes from the red blood cell. *Molecular and Biochemical Parasitology*, *243*, 111372. Available from: https://doi.org/10.1016/j.molbiopara.2021.111372

Birnbaum, J., Flemming, S., Reichard, N., Soares, A.B., Mesén-Ramírez, P., Jonscher, E. et al. (2017) A genetic system to study *Plasmodium falciparum* protein function. *Nature Methods*, *14*(4), 450–456. Available from: https://doi.org/10.1038/nmeth.4223

Black, C.G., Wu, T., Wang, L., Topolska, A.E. & Coppel, R.L. (2005) MSP8 is a non-essential merozoite surface protein in *Plasmodium falciparum*. *Molecular and Biochemical Parasitology*, *144*(1), 27–35. Available from: https://doi.org/10.1016/j.molbiopara.2005.06.010

Boysen, K.E. & Matuschewski, K. (2013) Inhibitor of cysteine proteases is critical for motility and infectivity of *Plasmodium* sporozoites. *mBio*, *4*(6), e00874-13. Available from: https://doi.org/10.1128/mBio.00874-13

Branon, T.C., Bosch, J.A., Sanchez, A.D., Udeshi, N.D., Svinkina, T., Carr, S.A. et al. (2018) Efficient proximity labeling in living cells and organisms with TurboID. *Nature Biotechnology*, *36*(9), 880–887. Available from: https://doi.org/10.1038/nbt.4201

Bruce, M.C., Carter, R.N., Nakamura, K., Aikawa, M. & Carter, R. (1994) Cellular location and temporal expression of the *Plasmodium falciparum* sexual stage antigen Pfs16. *Molecular and Biochemical Parasitology*, *65*(1), 11–22. Available from: https://doi.org/10.1016/0166-6851(94)90111-2

Charnaud, S.C., Dixon, M.W.A., Nie, C.Q., Chappell, L., Sanders, P.R., Nebl, T. et al. (2017) The exported chaperone Hsp70-x supports virulence functions for *Plasmodium falciparum* blood stage parasites. *PLoS ONE*, *12*(7), e0181656. Available from: https://doi.org/10.1371/journal.pone.0181656

Child, M.A., Harris, P.K., Collins, C.R., Withers-Martinez, C., Yeoh, S. & Blackman, M.J. (2013) Molecular determinants for subcellular trafficking of the malarial sheddase PfSUB2. *Traffic*, *14*(10), 1053–1064. Available from: https://doi.org/10.1111/tra.12092

Collins, C.R., Hackett, F., Atid, J., Tan, M.S.Y. & Blackman, M.J. (2017) The *Plasmodium falciparum* pseudoprotease SERA5 regulates the kinetics and efficiency of malaria parasite egress from host erythrocytes. *PLoS Pathogens*, *13*(7), e1006453. Available from: https://doi.org/10.1371/journal.ppat.1006453

Collins, C.R., Hackett, F., Howell, S.A., Snijders, A.P., Russell, M.R., Collinson, L.M. et al. (2020) The malaria parasite sheddase SUB2 governs host red blood cell membrane sealing at invasion. *eLife*, *9*, e61121. Available from: https://doi.org/10.7554/eLife.61121

Coombs, G.H., Goldberg, D.E., Klemba, M., Berry, C., Kay, J. & Mottram, J.C. (2001) Aspartic proteases of *Plasmodium falciparum* and other parasitic protozoa as drug targets. *Trends in Parasitology*, *17*(11), 532–537. Available from: https://doi.org/10.1016/s1471-4922(01)02037-2

Counihan, N.A., Chisholm, S.A., Bullen, H.E., Srivastava, A., Sanders, P.R., Jonsdottir, T.K. et al. (2017) *Plasmodium falciparum* parasites deploy RhopH2 into the host erythrocyte to obtain nutrients, grow and replicate. *eLife*, *6*, e23217. Available from: https://doi.org/10.7554/eLife.23217

Cowman, A.F., Berry, D. & Baum, J. (2012) The cellular and molecular basis for malaria parasite invasion of the human red blood cell. *The Journal of Cell Biology*, *198*(6), 961–971. Available from: https://doi.org/10.1083/jcb.201206112

Cowman, A.F., Tonkin, C.J., Tham, W.-H. & Duraisingh, M.T. (2017) The molecular basis of erythrocyte invasion by malaria parasites. *Cell Host & Microbe*, *22*(2), 232–245. Available from: https://doi.org/10.1016/j.chom.2017.07.003

Cox, J., Hein, M.Y., Luber, C.A., Paron, I., Nagaraj, N. & Mann, M. (2014) Accurate proteome-wide label-free quantification by delayed normalization and maximal peptide ratio extraction, termed MaxLFQ. *Molecular & Cellular Proteomics*, *13*(9), 2513–2526. Available from: https://doi.org/10.1074/mcp.M113.031591

Cox, J. & Mann, M. (2008) MaxQuant enables high peptide identification rates, individualized p.p.b.-range mass accuracies and proteome-wide protein quantification. *Nature Biotechnology*, *26*(12), 1367–1372. Available from: https://doi.org/10.1038/nbt.1511

Curtidor, H., Ocampo, M., Tovar, D., López, R., García, J., Valbuena, J. et al. (2004) Specific erythrocyte binding capacity and biological activity of *Plasmodium falciparum*-derived rhoptry-associated protein 1 peptides. *Vaccine*, *22*(8), 1054–1062. Available from: https://doi.org/10.1016/j.vaccine.2003.07.019

da Silva, F.L., Dixon, M.W.A., Stack, C.M., Teuscher, F., Taran, E., Jones, M.K. et al. (2016) A *Plasmodium falciparum* S33 proline aminopeptidase is associated with changes in erythrocyte deformability. *Experimental Parasitology*, *169*, 13–21. Available from: https://doi.org/10.1016/j.exppara.2016.06.013

de Koning-Ward, T.F., Gilson, P.R., Boddey, J.A., Rug, M., Smith, B.J., Papenfuss, A.T. et al. (2009) A newly discovered protein export machine in malaria parasites. *Nature*, *459*(7249), 945–949. Available from: https://doi.org/10.1038/nature08104

de Koning-Ward, T.F., Olivieri, A., Bertuccini, L., Hood, A., Silvestrini, F., Charvalias, K. et al. (2008) The role of osmiophilic bodies and Pfg377 expression in female gametocyte emergence and mosquito infectivity in the human malaria parasite *Plasmodium falciparum*. *Molecular Microbiology*, *67*(2), 278–290. Available from: https://doi.org/10.1111/j.1365-2958.2007.06039.x

Deligianni, E., Morgan, R.N., Bertuccini, L., Wirth, C.C., Silmon de Monerri, N.C., Spanos, L. et al. (2013) A perforin-like protein mediates disruption of the erythrocyte membrane during egress of *Plasmodium berghei* male gametocytes. *Cellular Microbiology*, *15*(8), 1438–1455. Available from: https://doi.org/10.1111/cmi.12131

Dixon, M.W.A., Kenny, S., McMillan, P.J., Hanssen, E., Trenholme, K.R., Gardiner, D.L. et al. (2011) Genetic ablation of a Maurer's cleft protein prevents assembly of the *Plasmodium falciparum* virulence complex. *Molecular Microbiology*, *81*(4), 982–993. Available from: https://doi.org/10.1111/j.1365-2958.2011.07740.x

Dvorin, J.D. & Goldberg, D.E. (2022) *Plasmodium* egress across the parasite life cycle. *Annual Review of Microbiology*, *76*, 67–90. Available from: https://doi.org/10.1146/annurev-micro-041320-020659

Eastman, R.T., Pattaradilokrat, S., Raj, D.K., Dixit, S., Deng, B., Miura, K. et al. (2013) A class of tricyclic compounds blocking malaria parasite oocyst development and transmission. *Antimicrobial Agents and Chemotherapy*, *57*(1), 425–435. Available from: https://doi.org/10.1128/AAC.00920-12

Ecker, A., Bushell, E.S.C., Tewari, R. & Sinden, R.E. (2008) Reverse genetics screen identifies six proteins important for malaria development in the mosquito. *Molecular Microbiology*, *70*(1), 209–220. Available from: https://doi.org/10.1111/j.1365-2958.2008.06407.x

Eksi, S., Haile, Y., Furuya, T., Ma, L., Su, X. & Williamson, K.C. (2005) Identification of a subtelomeric gene family expressed during the asexual-sexual stage transition in *Plasmodium falciparum*. *Molecular and Biochemical Parasitology*, *143*(1), 90–99. Available from: https://doi.org/10.1016/j.molbiopara.2005.05.010

Elsworth, B., Matthews, K., Nie, C.Q., Kalanon, M., Charnaud, S.C., Sanders, P.R. et al. (2014) PTEX is an essential nexus for protein export in malaria parasites. *Nature*, *511*(7511), 587–591. Available from: https://doi.org/10.1038/nature13555

Fischer, K., Marti, T., Rick, B., Johnson, D., Benting, J., Baumeister, S. et al. (1998) Characterization and cloning of the gene encoding the vacuolar membrane protein EXP-2 from *Plasmodium falciparum*. *Molecular and Biochemical Parasitology*, *92*(1), 47–57. Available from: https://doi.org/10.1016/s0166-6851(97)00224-7

Flieger, A., Frischknecht, F., Häcker, G., Hornef, M.W. & Pradel, G. (2018) Pathways of host cell exit by intracellular pathogens. *Microbial Cell*, *5*(12), 525–544. Available from: https://doi.org/10.15698/mic2018.12.659

Furuya, T., Mu, J., Hayton, K., Liu, A., Duan, J., Nkrumah, L. et al. (2005) Disruption of a *Plasmodium falciparum* gene linked to male sexual development causes early arrest in gametocytogenesis. *Proceedings of the National Academy of Sciences of the United States of America*, *102*(46), 16813–16818. Available from: https://doi.org/10.1073/pnas.0501858102

Goldberg, D.E. (2005) Hemoglobin degradation. *Current Topics in Microbiology and Immunology*, *295*, 275–291. Available from: https://doi.org/10.1007/3-540-29088-5_11

Goodman, C.D., Mollard, V., Louie, T., Holloway, G.A., Watson, K.G. & McFadden, G.I. (2014) Apicoplast acetyl Co-A carboxylase of the human malaria parasite is not targeted by cyclohexanedione herbicides. *International Journal for Parasitology*, *44*(5), 285–289. Available from: https://doi.org/10.1016/j.ijpara.2014.01.007

Grasso, F., Fratini, F., Albanese, T.G., Mochi, S., Ciardo, M., Pace, T. et al. (2022) Identification and preliminary characterization of *Plasmodium falciparum* proteins secreted upon gamete formation. *Scientific Reports*, *12*(1), 9592. Available from: https://doi.org/10.1038/s41598-022-13415-7

Grasso, F., Mochi, S., Fratini, F., Olivieri, A., Currà, C., Siden Kiamos, I. et al. (2020) A comprehensive gender-related secretome of *Plasmodium berghei* sexual stages. *Molecular & Cellular Proteomics*, *19*(12), 1986–1997. Available from: https://doi.org/10.1074/mcp.RA120.002212

Hallée, S., Thériault, C., Gagnon, D., Kehrer, J., Frischknecht, F., Mair, G.R. et al. (2018) Identification of a Golgi apparatus protein complex important for the asexual erythrocytic cycle of the malaria parasite *Plasmodium falciparum*. *Cellular Microbiology*, *20*(8), e12843. Available from: https://doi.org/10.1111/cmi.12843

Hallgren, J., Tsirigos, K.D., Pedersen, M.D., Almagro Armenteros, J.J., Marcatili, P., Nielsen, H. et al. (2022) DeepTMHMM predicts alpha and beta transmembrane proteins using deep neural networks. *BioRxiv Preprint*. Available from: https://doi.org/10.1101/2022.04.08.487609

Hentzschel, F., Mitesser, V., Fraschka, S.A.-K., Krzikalla, D., Carrillo, E.H., Berkhout, B. et al. (2020) Gene knockdown in malaria parasites via non-canonical RNAi. *Nucleic Acids Research*, *48*(1), e2. Available from: https://doi.org/10.1093/nar/gkz927

Hinds, L., Green, J.L., Knuepfer, E., Grainger, M. & Holder, A.A. (2009) Novel putative glycosylphosphatidylinositol-anchored micronemal antigen of *Plasmodium falciparum* that binds to erythrocytes. *Eukaryotic Cell*, *8*(12), 1869–1879. Available from: https://doi.org/10.1128/EC.00218-09

Hughes, C.S., Foehr, S., Garfield, D.A., Furlong, E.E., Steinmetz, L.M. & Krijgsveld, J. (2014) Ultrasensitive proteome analysis using paramagnetic bead technology. *Molecular Systems Biology*, *10*(10), 757. Available from: https://doi.org/10.15252/msb.20145625

Ifediba, T. & Vanderberg, J.P. (1981) Complete in vitro maturation of *Plasmodium falciparum* gametocytes. *Nature*, *294*(5839), 364–366. Available from: https://doi.org/10.1038/294364a0

Ito, D., Schureck, M.A. & Desai, S.A. (2017) An essential dual-function complex mediates erythrocyte invasion and channel-mediated nutrient uptake in malaria parasites. *eLife*, *6*, e23485. Available from: https://doi.org/10.7554/eLife.23485

Kadekoppala, M., Ogun, S.A., Howell, S., Gunaratne, R.S. & Holder, A.A. (2010) Systematic genetic analysis of the *Plasmodium falciparum* MSP7-like family reveals differences in protein expression, location, and importance in asexual growth of the blood-stage parasite. *Eukaryotic Cell*, *9*(7), 1064–1074. Available from: https://doi.org/10.1128/EC.00048-10

Kaneko, I., Iwanaga, S., Kato, T., Kobayashi, I. & Yuda, M. (2015) Genome-wide identification of the target genes of AP2-O, a *Plasmodium* AP2-family transcription factor. *PLoS Pathogens*, *11*(5), e1004905. Available from: https://doi.org/10.1371/journal.ppat.1004905

Kariuki, M.M., Kiaira, J.K., Mulaa, F.K., Mwangi, J.K., Wasunna, M.K. & Martin, S.K. (1998) *Plasmodium falciparum*: purification of the various gametocyte developmental stages from in vitro-cultivated parasites. *The American Journal of Tropical Medicine and Hygiene*, *59*(4), 505–508. Available from: https://doi.org/10.4269/ajtmh.1998.59.505

Kehrer, J., Frischknecht, F. & Mair, G.R. (2016) Proteomic analysis of the *Plasmodium berghei* gametocyte egressome and vesicular bioID of osmiophilic body proteins identifies merozoite TRAP-like protein (MTRAP) as an essential factor for parasite transmission. *Molecular & Cellular Proteomics*, *15*(9), 2852–2862. Available from: https://doi.org/10.1074/mcp.M116.058263

Kehrer, J., Singer, M., Lemgruber, L., Silva, P.A.G.C., Frischknecht, F. & Mair, G.R. (2016) A putative small solute transporter is responsible for the secretion of G377 and TRAP-containing secretory vesicles during *Plasmodium* gamete egress and sporozoite motility. *PLoS Pathogens*, *12*(7), e1005734. Available from: https://doi.org/10.1371/journal.ppat.1005734

Kenthirapalan, S., Tran, P.N., Kooij, T.W.A., Ridgway, M.C., Rauch, M., Brown, S.H.J. et al. (2020) Distinct adaptations of a gametocyte ABC transporter to murine and human *Plasmodium* parasites and its incompatibility in cross-species complementation. *International Journal for Parasitology*, *50*(6–7), 511–522. Available from: https://doi.org/10.1016/j.ijpara.2020.03.009

Khan, S.M., Kroeze, H., Franke-Fayard, B. & Janse, C.J. (2013) Standardization in generating and reporting genetically modified rodent malaria parasites: the RMgmDB database. *Methods in Molecular Biology*, *923*, 139–150. Available from: https://doi.org/10.1007/978-1-62703-026-7_9

Khosh-Naucke, M., Becker, J., Mesén-Ramírez, P., Kiani, P., Birnbaum, J., Fröhlke, U. et al. (2018) Identification of novel parasitophorous vacuole proteins in *P. falciparum* parasites using BioID. *International Journal of Medical Microbiology*, *308*(1), 13–24. Available from: https://doi.org/10.1016/j.ijmm.2017.07.007

Klemba, M., Gluzman, I. & Goldberg, D.E. (2004) A *Plasmodium falciparum* dipeptidyl aminopeptidase I participates in vacuolar hemoglobin degradation. *The Journal of Biological Chemistry*, *279*(41), 43000–43007. Available from: https://doi.org/10.1074/jbc.M408123200

Kongkasuriyachai, D., Fujioka, H. & Kumar, N. (2004) Functional analysis of *Plasmodium falciparum* parasitophorous vacuole membrane protein (Pfs16) during gametocytogenesis and gametogenesis by targeted gene disruption. *Molecular and Biochemical Parasitology*, *133*(2), 275–285. Available from: https://doi.org/10.1016/j.molbiopara.2003.10.014

Kou, X., Zheng, W., Du, F., Liu, F., Wang, M., Fan, Q. et al. (2016) Characterization of a *Plasmodium berghei* sexual stage antigen PbPH as a new candidate for malaria transmission-blocking vaccine. *Parasites & Vectors*, *9*, 190. Available from: https://doi.org/10.1186/s13071-016-1459-8

Kuehn, A. & Pradel, G. (2010) The coming-out of malaria gametocytes. *Journal of Biomedicine & Biotechnology*, *2010*, 976827. Available from: https://doi.org/10.1155/2010/976827

Kuehn, A., Simon, N. & Pradel, G. (2010) Family members stick together: multi-protein complexes of malaria parasites. *Medical Microbiology and Immunology*, *199*(3), 209–226. Available from: https://doi.org/10.1007/s00430-010-0157-y

Külzer, S., Gehde, N. & Przyborski, J.M. (2009) Return to sender: use of *Plasmodium* ER retrieval sequences to study protein transport in the infected erythrocyte and predict putative ER protein families. *Parasitology Research*, *104*(6), 1535–1541. Available from: https://doi.org/10.1007/s00436-009-1397-x

Lal, K., Delves, M.J., Bromley, E., Wastling, J.M., Tomley, F.M. & Sinden, R.E. (2009) *Plasmodium* male development gene-1 (mdv-1) is important for female sexual development and identifies a polarised plasma membrane during zygote development. *International Journal for Parasitology*, *39*(7), 755–761. Available from: https://doi.org/10.1016/j.ijpara.2008.11.008

Lanfrancotti, A., Bertuccini, L., Silvestrini, F. & Alano, P. (2007) *Plasmodium falciparum*: mRNA co-expression and protein co-localisation of two gene products upregulated in early gametocytes. *Experimental Parasitology*, *116*(4), 497–503. Available from: https://doi.org/10.1016/j.exppara.2007.01.021

Lasonder, E., Rijpma, S.R., van Schaijk, B.C.L., Hoeijmakers, W.A.M., Kensche, P.R., Gresnigt, M.S. et al. (2016) Integrated transcriptomic and proteomic analyses of *P. falciparum* gametocytes: molecular insight into sex-specific processes and translational repression. *Nucleic Acids Research*, *44*(13), 6087–6101. Available from: https://doi.org/10.1093/nar/gkw536

Lehmann, C., Heitmann, A., Mishra, S., Burda, P.-C., Singer, M., Prado, M. et al. (2014) A cysteine protease inhibitor of *Plasmodium berghei* is essential for exo-erythrocytic development. *PLoS Pathogens*, *10*(8), e1004336. Available from: https://doi.org/10.1371/journal.ppat.1004336

Lin, J.-W., Spaccapelo, R., Schwarzer, E., Sajid, M., Annoura, T., Deroost, K. et al. (2015) Replication of *Plasmodium* in reticulocytes can occur without hemozoin formation, resulting in chloroquine resistance. *The Journal of Experimental Medicine*, *212*(6), 893–903. Available from: https://doi.org/10.1084/jem.20141731

López-Barragán, M.J., Lemieux, J., Quiñones, M., Williamson, K.C., Molina-Cruz, A., Cui, K. et al. (2011) Directional gene expression and antisense transcripts in sexual and asexual stages of *Plasmodium falciparum*. *BMC Genomics*, *12*, 587. Available from: https://doi.org/10.1186/1471-2164-12-587

Maier, A.G., Rug, M., O'Neill, M.T., Brown, M., Chakravorty, S., Szestak, T. et al. (2008) Exported proteins required for virulence and rigidity of *Plasmodium falciparum*-infected human erythrocytes. *Cell*, *134*(1), 48–61. Available from: https://doi.org/10.1016/j.cell.2008.04.051

Marin-Mogollon, C., van de Vegte-Bolmer, M., van Gemert, G.-J., van Pul, F.J.A., Ramesar, J., Othman, A.S. et al. (2018) The *Plasmodium falciparum* male gametocyte protein P230p, a paralog of P230, is vital for ookinete formation and mosquito transmission. *Scientific Reports*, *8*(1), 14902. Available from: https://doi.org/10.1038/s41598-018-33236-x

Matz, J.M. & Matuschewski, K. (2018) An in silico down-scaling approach uncovers novel constituents of the *Plasmodium*-containing vacuole. *Scientific Reports*, *8*(1), 14055. Available from: https://doi.org/10.1038/s41598-018-32471-6

Mbengue, A., Audiger, N., Vialla, E., Dubremetz, J.-F. & Braun-Breton, C. (2013) Novel *Plasmodium falciparum* Maurer's clefts protein families implicated in the release of infectious merozoites. *Molecular Microbiology*, *88*(2), 425–442. Available from: https://doi.org/10.1111/mmi.12193

Mesén-Ramírez, P., Bergmann, B., Tran, T.T., Garten, M., Stäcker, J., Naranjo-Prado, I. et al. (2019) EXP1 is critical for nutrient uptake across the parasitophorous vacuole membrane of malaria parasites. *PLoS Biology*, *17*(9), e3000473. Available from: https://doi.org/10.1371/journal.pbio.3000473

Mesén-Ramírez, P., Reinsch, F., Blancke Soares, A., Bergmann, B., Ullrich, A.-K., Tenzer, S. et al. (2016) Stable translocation intermediates jam global protein export in *Plasmodium falciparum* parasites and link the PTEX component EXP2 with translocation activity. *PLoS Pathogens*, *12*(5), e1005618. Available from: https://doi.org/10.1371/journal.ppat.1005618

Molina-Franky, J., Patarroyo, M.E., Kalkum, M. & Patarroyo, M.A. (2022) The cellular and molecular interaction between erythrocytes and *Plasmodium falciparum* merozoites. *Frontiers in Cellular and Infection Microbiology*, *12*, 816574. Available from: https://doi.org/10.3389/fcimb.2022.816574

Morahan, B.J., Strobel, C., Hasan, U., Czesny, B., Mantel, P.-Y., Marti, M. et al. (2011) Functional analysis of the exported type IV HSP40 protein PfGECO in *Plasmodium falciparum* gametocytes. *Eukaryotic Cell*, *10*(11), 1492–1503. Available from: https://doi.org/10.1128/EC.05155-11

Mukherjee, S., Nasamu, A.S., Rubiano, K.C. & Goldberg, D.E. (2023) Activation of the *Plasmodium* egress effector subtilisin-like protease 1 is mediated by plasmepsin X destruction of the prodomain. *mBio*, *14*(2), e0067323. Available from: https://doi.org/10.1128/mbio.00673-23

Musabyimana, J.P., Distler, U., Sassmannshausen, J., Berks, C., Manti, J., Bennink, S. et al. (2022) *Plasmodium falciparum* S-Adenosylmethionine synthetase is essential for parasite survival through a complex interaction network with cytoplasmic and nuclear proteins. *Microorganisms*, *10*(7), 1419. Available from: https://doi.org/10.3390/microorganisms10071419

Muthui, M.K., Takashima, E., Omondi, B.R., Kinya, C., Muasya, W.I., Nagaoka, H. et al. (2021) Characterization of naturally acquired immunity to a panel of antigens expressed in mature *P. falciparum* gametocytes. *Frontiers in Cellular and Infection Microbiology*, *11*, 774537. Available from: https://doi.org/10.3389/fcimb.2021.774537

Nasamu, A.S., Glushakova, S., Russo, I., Vaupel, B., Oksman, A., Kim, A.S. et al. (2017) Plasmepsins IX and X are essential and druggable mediators of malaria parasite egress and invasion. *Science*, *358*(6362), 518–522. Available from: https://doi.org/10.1126/science.aan1478

Nasamu, A.S., Polino, A.J., Istvan, E.S. & Goldberg, D.E. (2020) Malaria parasite plasmepsins: more than just plain old degradative pepsins. *The Journal of Biological Chemistry*, *295*(25), 8425–8441. Available from: https://doi.org/10.1074/jbc.REV120.009309

Ngwa, C.J., Kiesow, M.J., Papst, O., Orchard, L.M., Filarsky, M., Rosinski, A.N. et al. (2017) Transcriptional profiling defines histone acetylation as a regulator of gene expression during human-to-mosquito transmission of the malaria parasite *Plasmodium falciparum*. *Frontiers*

in Cellular and Infection Microbiology, *7*, 320. Available from: https://doi.org/10.3389/fcimb.2017.00320

Ntumngia, F.B., Bouyou-Akotet, M.K., Uhlemann, A.-C., Mordmüller, B., Kremsner, P.G. & Kun, J.F.J. (2004) Characterisation of a tryptophan-rich *Plasmodium falciparum* antigen associated with merozoites. *Molecular and Biochemical Parasitology*, *137*(2), 349–353. Available from: https://doi.org/10.1016/j.molbiopara.2004.06.008

Nunes, M.C., Okada, M., Scheidig-Benatar, C., Cooke, B.M. & Scherf, A. (2010) *Plasmodium falciparum* FIKK kinase members target distinct components of the erythrocyte membrane. *PLoS ONE*, *5*(7), e11747. Available from: https://doi.org/10.1371/journal.pone.0011747

Okuda, S., Watanabe, Y., Moriya, Y., Kawano, S., Yamamoto, T., Matsumoto, M. et al. (2017) jPOSTrepo: an international standard data repository for proteomes. *Nucleic Acids Research*, *45*(D1), D1107–D1111. Available from: https://doi.org/10.1093/nar/gkw1080

Olivieri, A., Bertuccini, L., Deligianni, E., Franke-Fayard, B., Currà, C., Siden-Kiamos, I. et al. (2015) Distinct properties of the egress-related osmiophilic bodies in male and female gametocytes of the rodent malaria parasite *Plasmodium berghei*. *Cellular Microbiology*, *17*(3), 355–368. Available from: https://doi.org/10.1111/cmi.12370

Omara-Opyene, A.L., Moura, P.A., Sulsona, C.R., Bonilla, J.A., Yowell, C.A., Fujioka, H. et al. (2004) Genetic disruption of the *Plasmodium falciparum* digestive vacuole plasmepsins demonstrates their functional redundancy. *The Journal of Biological Chemistry*, *279*(52), 54088–54096. Available from: https://doi.org/10.1074/jbc.M409605200

Pace, T., Grasso, F., Camarda, G., Suarez, C., Blackman, M.J., Ponzi, M. et al. (2019) The *Plasmodium berghei* serine protease PbSUB1 plays an important role in male gamete egress. *Cellular Microbiology*, *21*(7), e13028. Available from: https://doi.org/10.1111/cmi.13028

Pandey, K.C., Singh, N., Arastu-Kapur, S., Bogyo, M. & Rosenthal, P.J. (2006) Falstatin, a cysteine protease inhibitor of *Plasmodium falciparum*, facilitates erythrocyte invasion. *PLoS Pathogens*, *2*(11), e117. Available from: https://doi.org/10.1371/journal.ppat.0020117

Pasini, E.M., Braks, J.A., Fonager, J., Klop, O., Aime, E., Spaccapelo, R. et al. (2013) Proteomic and genetic analyses demonstrate that *Plasmodium berghei* blood stages export a large and diverse repertoire of proteins. *Molecular & Cellular Proteomics*, *12*(2), 426–448. Available from: https://doi.org/10.1074/mcp.M112.021238

Petersen, T.N., Brunak, S., von Heijne, G. & Nielsen, H. (2011) SignalP 4.0: discriminating signal peptides from transmembrane regions. *Nature Methods*, *8*(10), 785–786. Available from: https://doi.org/10.1038/nmeth.1701

Pino, P., Caldelari, R., Mukherjee, B., Vahokoski, J., Klages, N., Maco, B. et al. (2017) A multistage antimalarial targets the plasmepsins IX and X essential for invasion and egress. *Science*, *358*(6362), 522–528. Available from: https://doi.org/10.1126/science.aaf8675

Ponzi, M., Sidén-Kiamos, I., Bertuccini, L., Currà, C., Kroeze, H., Camarda, G. et al. (2009) Egress of *Plasmodium berghei* gametes from their host erythrocyte is mediated by the MDV-1/PEG3 protein. *Cellular Microbiology*, *11*(8), 1272–1288. Available from: https://doi.org/10.1111/j.1462-5822.2009.01331.x

Pradel, G. (2007) Proteins of the malaria parasite sexual stages: expression, function and potential for transmission blocking strategies. *Parasitology*, *134*, 1911–1929. Available from: https://doi.org/10.1017/S0031182007003381

Pradel, G., Hayton, K., Aravind, L., Iyer, L.M., Abrahamsen, M.S., Bonawitz, A. et al. (2004) A multidomain adhesion protein family expressed in *Plasmodium falciparum* is essential for transmission to the mosquito. *The Journal of Experimental Medicine*, *199*(11), 1533–1544. Available from: https://doi.org/10.1084/jem.20031274

Putrianti, E.D., Schmidt-Christensen, A., Arnold, I., Heussler, V.T., Matuschewski, K. & Silvie, O. (2010) The *Plasmodium* serine-type SERA proteases display distinct expression patterns and non-essential in vivo roles during life cycle progression of the malaria parasite. *Cellular Microbiology*, *12*(6), 725–739. Available from: https://doi.org/10.1111/j.1462-5822.2009.01419.x

Roling, L., Flammersfeld, A., Pradel, G. & Bennink, S. (2022) The WD40-protein PfWLP1 ensures stability of the PfCCp-based adhesion protein complex in *Plasmodium falciparum* gametocytes. *Frontiers in Cellular and Infection Microbiology*, *12*, 942364. Available from: https://doi.org/10.3389/fcimb.2022.942364

Rosenthal, P.J. (2002) Hydrolysis of erythrocyte proteins by proteases of malaria parasites. *Current Opinion in Hematology*, *9*(2), 140–145. Available from: https://doi.org/10.1097/00062752-200203000-00010

Roux, K.J., Kim, D.I., Burke, B. & May, D.G. (2018) BioID: a screen for protein-protein interactions. *Current Protocols in Protein Science*, *91*, 19.23.1–19.23.15. Available from: https://doi.org/10.1002/cpps.51

Ruecker, A., Shea, M., Hackett, F., Suarez, C., Hirst, E.M.A., Milutinovic, K. et al. (2012) Proteolytic activation of the essential parasitophorous vacuole cysteine protease SERA6 accompanies malaria parasite egress from its host erythrocyte. *The Journal of Biological Chemistry*, *287*(45), 37949–37963. Available from: https://doi.org/10.1074/jbc.M112.400820

Sala, K.A., Nishiura, H., Upton, L.M., Zakutansky, S.E., Delves, M.J., Iyori, M. et al. (2015) The *Plasmodium berghei* sexual stage antigen PSOP12 induces anti-malarial transmission blocking immunity both in vivo and in vitro. *Vaccine*, *33*(3), 437–445. Available from: https://doi.org/10.1016/j.vaccine.2014.11.038

Sanchez, C.P., Dave, A., Stein, W.D. & Lanzer, M. (2010) Transporters as mediators of drug resistance in *Plasmodium falciparum*. *International Journal for Parasitology*, *40*(10), 1109–1118. Available from: https://doi.org/10.1016/j.ijpara.2010.04.001

Sanders, P.R., Gilson, P.R., Cantin, G.T., Greenbaum, D.C., Nebl, T., Carucci, D.J. et al. (2005) Distinct protein classes including novel merozoite surface antigens in raft-like membranes of *Plasmodium falciparum*. *The Journal of Biological Chemistry*, *280*(48), 40169–40176. Available from: https://doi.org/10.1074/jbc.M509631200

Sanderson, T. & Rayner, J.C. (2017) PhenoPlasm: a database of disruption phenotypes for malaria parasite genes. *Wellcome Open Research*, *2*, 45. Available from: https://doi.org/10.12688/wellcomeopenres.11896.2

Sassmannshausen, J., Pradel, G. & Bennink, S. (2020) Perforin-like proteins of apicomplexan parasites. *Frontiers in Cellular and Infection Microbiology*, *10*, 578883. Available from: https://doi.org/10.3389/fcimb.2020.578883

Scherf, A., Carter, R., Petersen, C., Alano, P., Nelson, R., Aikawa, M. et al. (1992) Gene inactivation of Pf11-1 of *Plasmodium falciparum* by chromosome breakage and healing: identification of a gametocyte-specific protein with a potential role in gametogenesis. *The EMBO Journal*, *11*(6), 2293–2301. Available from: https://doi.org/10.1002/j.1460-2075.1992.tb05288.x

Schindelin, J., Arganda-Carreras, I., Frise, E., Kaynig, V., Longair, M., Pietzsch, T. et al. (2012) Fiji: an open-source platform for biological-image analysis. *Nature Methods*, *9*, 676–682. Available from: https://doi.org/10.1038/nmeth.2019

Scholz, S.M., Simon, N., Lavazec, C., Dude, M.-A., Templeton, T.J. & Pradel, G. (2008) PfCCp proteins of *Plasmodium falciparum*: gametocyte-specific expression and role in complement-mediated inhibition of exflagellation. *International Journal for Parasitology*, *38*(3–4), 327–340. Available from: https://doi.org/10.1016/j.ijpara.2007.08.009

Schwach, F., Bushell, E., Gomes, A.R., Anar, B., Girling, G., Herd, C. et al. (2015) PlasmoGEM, a database supporting a community resource for large-scale experimental genetics in malaria parasites. *Nucleic Acids Research*, *43*, D1176–D1182. Available from: https://doi.org/10.1093/nar/gku1143

Severini, C., Silvestrini, F., Sannella, A., Barca, S., Gradoni, L. & Alano, P. (1999) The production of the osmiophilic body protein Pfg377 is associated with stage of maturation and sex in *Plasmodium falciparum*

gametocytes. *Molecular and Biochemical Parasitology*, *100*(2), 247–252. Available from: https://doi.org/10.1016/s0166-6851(99)00050-x

Sherling, E.S., Knuepfer, E., Brzostowski, J.A., Miller, L.H., Blackman, M.J. & van Ooij, C. (2017) The *Plasmodium falciparum* rhoptry protein RhopH3 plays essential roles in host cell invasion and nutrient uptake. *eLife*, *6*, e23239. Available from: https://doi.org/10.7554/eLife.23239

Siddiqui, G., Proellochs, N.I. & Cooke, B.M. (2020) Identification of essential exported *Plasmodium falciparum* protein kinases in malaria-infected red blood cells. *British Journal of Haematology*, *188*(5), 774–783. Available from: https://doi.org/10.1111/bjh.16219

Sielaff, M., Kuharev, J., Bohn, T., Hahlbrock, J., Bopp, T., Tenzer, S. et al. (2017) Evaluation of FASP, SP3, and iST protocols for proteomic sample preparation in the low microgram range. *Journal of Proteome Research*, *16*(11), 4060–4072. Available from: https://doi.org/10.1021/acs.jproteome.7b00433

Sijwali, P.S., Koo, J., Singh, N. & Rosenthal, P.J. (2006) Gene disruptions demonstrate independent roles for the four falcipain cysteine proteases of *Plasmodium falciparum*. *Molecular and Biochemical Parasitology*, *150*(1), 96–106. Available from: https://doi.org/10.1016/j.molbiopara.2006.06.013

Silmon de Monerri, N.C., Flynn, H.R., Campos, M.G., Hackett, F., Koussis, K., Withers-Martinez, C. et al. (2011) Global identification of multiple substrates for *Plasmodium falciparum* SUB1, an essential malarial processing protease. *Infection and Immunity*, *79*(3), 1086–1097. Available from: https://doi.org/10.1128/IAI.00902-10

Silvestrini, F., Bozdech, Z., Lanfrancotti, A., Di Giulio, E., Bultrini, E., Picci, L. et al. (2005) Genome-wide identification of genes upregulated at the onset of gametocytogenesis in *Plasmodium falciparum*. *Molecular and Biochemical Parasitology*, *143*(1), 100–110. Available from: https://doi.org/10.1016/j.molbiopara.2005.04.015

Silvestrini, F., Lasonder, E., Olivieri, A., Camarda, G., van Schaijk, B., Sanchez, M. et al. (2010) Protein export marks the early phase of gametocytogenesis of the human malaria parasite *Plasmodium falciparum*. *Molecular & Cellular Proteomics*, *9*(7), 1437–1448. Available from: https://doi.org/10.1074/mcp.M900479-MCP200

Simmons, D., Woollett, G., Bergin-Cartwright, M., Kay, D. & Scaife, J. (1987) A malaria protein exported into a new compartment within the host erythrocyte. *The EMBO Journal*, *6*(2), 485–491. Available from: https://doi.org/10.1002/j.1460-2075.1987.tb04779.x

Simon, N., Kuehn, A., Williamson, K.C. & Pradel, G. (2016) Adhesion protein complexes of malaria gametocytes assemble following parasite transmission to the mosquito. *Parasitology International*, *65*(1), 27–30. Available from: https://doi.org/10.1016/j.parint.2015.09.007

Simon, N., Scholz, S.M., Moreira, C.K., Templeton, T.J., Kuehn, A., Dude, M.-A. et al. (2009) Sexual stage adhesion proteins form multiprotein complexes in the malaria parasite *Plasmodium falciparum*. *The Journal of Biological Chemistry*, *284*(21), 14537–14546. Available from: https://doi.org/10.1074/jbc.M808472200

Sinden, R.E. (1982) Gametocytogenesis of *Plasmodium falciparum* in vitro: an electron microscopic study. *Parasitology*, *84*(1), 1–11. Available from: https://doi.org/10.1017/s003118200005160x

Siqueira-Neto, J.L., Debnath, A., McCall, L.-I., Bernatchez, J.A., Ndao, M., Reed, S.L. et al. (2018) Cysteine proteases in protozoan parasites. *PLoS Neglected Tropical Diseases*, *12*(8), e0006512. Available from: https://doi.org/10.1371/journal.pntd.0006512

Slavic, K., Straschil, U., Reininger, L., Doerig, C., Morin, C., Tewari, R. et al. (2010) Life cycle studies of the hexose transporter of *Plasmodium* species and genetic validation of their essentiality. *Molecular Microbiology*, *75*(6), 1402–1413. Available from: https://doi.org/10.1111/j.1365-2958.2010.07060.x

Sologub, L., Kuehn, A., Kern, S., Przyborski, J., Schillig, R. & Pradel, G. (2011) Malaria proteases mediate inside-out egress of gametocytes from red blood cells following parasite transmission to the mosquito. *Cellular Microbiology*, *13*(6), 897–912. Available from: https://doi.org/10.1111/j.1462-5822.2011.01588.x

Spaccapelo, R., Janse, C.J., Caterbi, S., Franke-Fayard, B., Bonilla, J.A., Syphard, L.M. et al. (2010) Plasmepsin 4-deficient *Plasmodium berghei* are virulence attenuated and induce protective immunity against experimental malaria. *The American Journal of Pathology*, *176*(1), 205–217. Available from: https://doi.org/10.2353/ajpath.2010.090504

Spycher, C., Rug, M., Pachlatko, E., Hanssen, E., Ferguson, D., Cowman, A.F. et al. (2008) The Maurer's cleft protein MAHRP1 is essential for trafficking of PfEMP1 to the surface of *Plasmodium falciparum*-infected erythrocytes. *Molecular Microbiology*, *68*(5), 1300–1314. Available from: https://doi.org/10.1111/j.1365-2958.2008.06235.x

Stallmach, R., Kavishwar, M., Withers-Martinez, C., Hackett, F., Collins, C.R., Howell, S.A. et al. (2015) *Plasmodium falciparum* SERA5 plays a non-enzymatic role in the malarial asexual blood-stage lifecycle. *Molecular Microbiology*, *96*(2), 368–387. Available from: https://doi.org/10.1111/mmi.12941

Suárez-Cortés, P., Sharma, V., Bertuccini, L., Costa, G., Bannerman, N.-L., Sannella, A.R. et al. (2016) Comparative proteomics and functional analysis reveal a role of *Plasmodium falciparum* osmiophilic bodies in malaria parasite transmission. *Molecular & Cellular Proteomics*, *15*(10), 3243–3255. Available from: https://doi.org/10.1074/mcp.M116.060681

Suaréz-Cortés, P., Silvestrini, F. & Alano, P. (2014) A fast, non-invasive, quantitative staining protocol provides insights in *Plasmodium falciparum* gamete egress and in the role of osmiophilic bodies. *Malaria Journal*, *13*, 389. Available from: https://doi.org/10.1186/1475-2875-13-389

Szklarczyk, D., Gable, A.L., Lyon, D., Junge, A., Wyder, S., Huerta-Cepas, J. et al. (2019) STRING v11: protein-protein association networks with increased coverage, supporting functional discovery in genome-wide experimental datasets. *Nucleic Acids Research*, *47*(D1), D607–D613. Available from: https://doi.org/10.1093/nar/gky1131

Tachibana, M., Iriko, H., Baba, M., Torii, M. & Ishino, T. (2021) PSOP1, putative secreted ookinete protein 1, is localized to the micronemes of *Plasmodium yoelii* and *P. berghei* ookinetes. *Parasitology International*, *84*, 102407. Available from: https://doi.org/10.1016/j.parint.2021.102407

Tachibana, M., Ishino, T., Tsuboi, T. & Torii, M. (2018) The *Plasmodium yoelii* microgamete surface antigen (PyMiGS) induces anti-malarial transmission blocking immunity that reduces microgamete motility/release from activated male gametocytes. *Vaccine*, *36*(49), 7463–7471. Available from: https://doi.org/10.1016/j.vaccine.2018.10.067

Talman, A.M., Lacroix, C., Marques, S.R., Blagborough, A.M., Carzaniga, R., Ménard, R. et al. (2011) PbGEST mediates malaria transmission to both mosquito and vertebrate host. *Molecular Microbiology*, *82*(2), 462–474. Available from: https://doi.org/10.1111/j.1365-2958.2011.07823.x

Tan, M.S.Y. & Blackman, M.J. (2021) Malaria parasite egress at a glance. *Journal of Cell Science*, *134*(5), jcs257345. Available from: https://doi.org/10.1242/jcs.257345

Tan, M.S.Y., Koussis, K., Withers-Martinez, C., Howell, S.A., Thomas, J.A., Hackett, F. et al. (2021) Autocatalytic activation of a malarial egress protease is druggable and requires a protein cofactor. *The EMBO Journal*, *40*(11), e107226. Available from: https://doi.org/10.15252/embj.2020107226

Tanaka, T.Q., Deu, E., Molina-Cruz, A., Ashburne, M.J., Ali, O., Suri, A. et al. (2013) *Plasmodium* dipeptidyl aminopeptidases as malaria transmission-blocking drug targets. *Antimicrobial Agents and Chemotherapy*, *57*(10), 4645–4652. Available from: https://doi.org/10.1128/AAC.02495-12

Thomas, J.A., Tan, M.S.Y., Bisson, C., Borg, A., Umrekar, T.R., Hackett, F. et al. (2018) A protease cascade regulates release of the human malaria parasite *Plasmodium falciparum* from host red blood cells. *Nature Microbiology*, *3*(4), 447–455. Available from: https://doi.org/10.1038/s41564-018-0111-0

Thumuluri, V., Almagro Armenteros, J.J., Johansen, A.R., Nielsen, H. & Winther, O. (2022) DeepLoc 2.0: multi-label subcellular localization prediction using protein language models. *Nucleic Acids Research*, *50*, W228–W234. Available from: https://doi.org/10.1093/nar/gkac278

Tran, P.N., Brown, S.H.J., Mitchell, T.W., Matuschewski, K., McMillan, P.J., Kirk, K. et al. (2014) A female gametocyte-specific ABC transporter plays a role in lipid metabolism in the malaria parasite. *Nature Communications*, *5*, 4773. Available from: https://doi.org/10.1038/ncomms5773

Trenholme, K.R., Brown, C.L., Skinner-Adams, T.S., Stack, C., Lowther, J., To, J. et al. (2010) Aminopeptidases of malaria parasites: new targets for chemotherapy. *Infectious Disorders Drug Targets*, *10*(3), 217–225. Available from: https://doi.org/10.2174/187152610791163363

Uzureau, P., Barale, J.-C., Janse, C.J., Waters, A.P. & Breton, C.B. (2004) Gene targeting demonstrates that the *Plasmodium berghei* subtilisin PbSUB2 is essential for red cell invasion and reveals spontaneous genetic recombination events. *Cellular Microbiology*, *6*(1), 65–78. Available from: https://doi.org/10.1046/j.1462-5822.2003.00343.x

van Dijk, M.R., Janse, C.J., Thompson, J., Waters, A.P., Braks, J.A., Dodemont, H.J. et al. (2001) A central role for P48/45 in malaria parasite male gamete fertility. *Cell*, *104*(1), 153–164. Available from: https://doi.org/10.1016/s0092-8674(01)00199-4

Vincensini, L., Fall, G., Berry, L., Blisnick, T. & Braun Breton, C. (2008) The RhopH complex is transferred to the host cell cytoplasm following red blood cell invasion by *Plasmodium falciparum*. *Molecular and Biochemical Parasitology*, *160*(2), 81–89. Available from: https://doi.org/10.1016/j.molbiopara.2008.04.002

Vizcaíno, J.A., Côté, R.G., Csordas, A., Dianes, J.A., Fabregat, A., Foster, J.M. et al. (2013) The PRoteomics IDEntifications (PRIDE) database and associated tools: status in 2013. *Nucleic Acids Research*, *41*, D1063–D1069. Available from: https://doi.org/10.1093/nar/gks1262

Warncke, J.D., Passecker, A., Kipfer, E., Brand, F., Pérez-Martínez, L., Proellochs, N.I. et al. (2020) The PHIST protein GEXP02 targets the host cytoskeleton during sexual development of *Plasmodium falciparum*. *Cellular Microbiology*, *22*(2), e13123. Available from: https://doi.org/10.1111/cmi.13123

Wass, M.N., Stanway, R., Blagborough, A.M., Lal, K., Prieto, J.H., Raine, D. et al. (2012) Proteomic analysis of *Plasmodium* in the mosquito: progress and pitfalls. *Parasitology*, *139*(9), 1131–1145. Available from: https://doi.org/10.1017/S0031182012000133

Williamson, K.C., Keister, D.B., Muratova, O. & Kaslow, D.C. (1995) Recombinant Pfs230, a *Plasmodium falciparum* gametocyte protein, induces antisera that reduce the infectivity of *Plasmodium falciparum* to mosquitoes. *Molecular and Biochemical Parasitology*, *75*(1), 33–42. Available from: https://doi.org/10.1016/0166-6851(95)02507-3

Wirth, C.C., Glushakova, S., Scheuermayer, M., Repnik, U., Garg, S., Schaack, D. et al. (2014) Perforin-like protein PPLP2 permeabilizes the red blood cell membrane during egress of *Plasmodium falciparum* gametocytes. *Cellular Microbiology*, *16*(5), 709–733. Available from: https://doi.org/10.1111/cmi.12288

Wirth, C.C. & Pradel, G. (2012) Molecular mechanisms of host cell egress by malaria parasites. *International Journal of Medical Microbiology*, *302*, 4–5. Available from: https://doi.org/10.1016/j.ijmm.2012.07.003

World Health Organization. (2022) *WHO word malaria report 2022*. Geneva, Switzerland: WHO.

Yeoh, S., O'Donnell, R.A., Koussis, K., Dluzewski, A.R., Ansell, K.H., Osborne, S.A. et al. (2007) Subcellular discharge of a serine protease mediates release of invasive malaria parasites from host erythrocytes. *Cell*, *131*(6), 1072–1083. Available from: https://doi.org/10.1016/j.cell.2007.10.049

Zhang, M., Wang, C., Otto, T.D., Oberstaller, J., Liao, X., Adapa, S.R. et al. (2018) Uncovering the essential genes of the human malaria parasite *Plasmodium falciparum* by saturation mutagenesis. *Science*, *360*, 6388. Available from: https://doi.org/10.1126/science.aap7847

SUPPORTING INFORMATION

Additional supporting information can be found online in the Supporting Information section at the end of this article.

How to cite this article: Sassmannshausen, J., Bennink, S., Distler, U., Küchenhoff, J., Minns, A. M., Lindner, S. E., Burda, P-C., Tenzer, S., Gilberger, T. W. & Pradel, G. (2023). Comparative proteomics of vesicles essential for the egress of *Plasmodium falciparum* gametocytes from red blood cells. *Molecular Microbiology*, *00*, 1–22. https://doi.org/10.1111/mmi.15125